Copy 151
RM L55G18

NACA RM L55G18

NACA

RESEARCH MEMORANDUM

THEORETICAL ANALYSIS OF THE LONGITUDINAL BEHAVIOR OF AN AUTOMATICALLY CONTROLLED SUPERSONIC INTERCEPTOR DURING THE ATTACK PHASE AGAINST MANEUVERING AND NONMANEUVERING TARGETS

By C. H. Woodling and Ordway B. Gates, Jr.

Langley Aeronautical Laboratory
Langley Field, Va.

Aircraft Armaments, Inc.
Cockeysville, Maryland

NATIONAL ADVISORY COMMITTEE FOR AERONAUTICS

WASHINGTON

October 3, 1955

NATIONAL ADVISORY COMMITTEE FOR AERONAUTICS

RESEARCH MEMORANDUM

THEORETICAL ANALYSIS OF THE LONGITUDINAL BEHAVIOR OF AN AUTOMATICALLY CONTROLLED SUPERSONIC INTERCEPTOR DURING THE ATTACK PHASE AGAINST MANEUVERING AND NONMANEUVERING TARGETS

By C. H. Woodling and Ordway B. Gates, Jr.

SUMMARY

A theoretical analysis has been made of the longitudinal behavior of an automatically controlled supersonic interceptor during the attack phase of the interception problem. Attack runs were computed for a nonmaneuvering target, and for a target which had a constant acceleration normal to its flight path. First-order lead collision navigation was assumed in the investigation, and characteristics of this navigation when used against a maneuvering target are discussed. The flight path of the interceptor was controlled by commanding either a pitching velocity or normal acceleration proportional to the vertical steering error. Computed attack runs are presented which demonstrate some of the advantages and disadvantages of using high gain or integration in the tracking system to minimize or eliminate bias errors in the system which result from target acceleration or interceptor trim changes.

Results are also presented which show the effect of limits on the rate of control deflection, and several means of counteracting the effects of this limiting are discussed.

INTRODUCTION

The Langley Laboratory of the National Advisory Committee for Aeronautics is conducting an analytical study of automatically controlled, rocket firing, supersonic interceptors during the attack phase of the interception problem. The term "attack phase" refers to that phase of the interception which exists subsequent to the time at which the interceptor's radar becomes locked on to a specified target. Results have been reported in reference 1 for the case in which the interceptor locked onto a nonmaneuvering target with an initial vertical tracking error. Only longitudinal maneuvers of the interceptor were necessary to carry out the desired interception. Lead collision navigation was used in this reference, and the tie-in between the radar-guidance computer and the interceptor was a command on pitching velocity proportional to the existing error in the interceptor's flight path. The interceptor considered in reference 1 has a notched delta wing of aspect ratio 3.2 with 55° sweepback of the leading edge. A more detailed discussion of this configuration can be found in reference 2.

The present paper is concerned primarily with the longitudinal attack performance of the interceptor of reference 1 against a target which is assumed to be maneuvering with a constant normal acceleration. The interceptor is initially in level flight at 50,000 feet at a Mach number of 2.2. The target is initially in level flight at a Mach number of 1.4, flying toward the interceptor at various altitudes above 50,000 feet. No consideration is given to the effect of altitude changes on the interceptor's longitudinal behavior during the attack runs.

The results of this investigation are presented, for the most part, in the form of interceptor and kinematic responses subsequent to radar lock-on, which were computed on the Reeves Electronic Analog Computer (REAC).

SYMBOLS

I_Y	moment of inertia about Y-axis, slug-ft^2
m	mass of airplane, slugs
$\bar{c}$	mean aerodynamic chord, ft
S	wing area, sq ft
q	dynamic pressure, lb/sq ft
V	forward velocity, ft/sec
M	Mach number
n	normal acceleration, number of g
Δn	change in normal acceleration, number of g
g	acceleration due to gravity, ft/sec^2

q	$\dot{\theta}\bar{c}/2V$ when used as a subscript
θ	angle of pitch, radians unless otherwise specified
α	angle of attack, radians unless otherwise specified
γ	flight-path angle ($\gamma = \theta - \alpha$), radians unless otherwise specified
u or ΔV	change in forward velocity, ft/sec
u'	relative change in forward velocity, $\frac{u}{V}$ or $\frac{\Delta V}{V}$
δ_e	elevator deflection, radians unless otherwise specified

$\delta_e' = -\delta_e$

t	time, sec
L	lift, lb
C_L	trim lift coefficient, $\frac{\text{Lift}}{qS}$
D	drag, lb
C_D	trim drag coefficient, $\frac{\text{Drag}}{qS}$
M'	pitching moment, lb-ft
C_m	pitching-moment coefficient, $\frac{\text{Pitching moment}}{qS\bar{c}}$

$C_{L_{\delta_e}} = \frac{\partial C_L}{\partial \delta_e}$, per radian

$C_{L_\alpha} = \frac{\partial C_L}{\partial \alpha}$, per radian

$C_{m_{\delta_e}} = \frac{\partial C_m}{\partial \delta_e}$, per radian

$C_{m_\alpha} = \frac{\partial C_m}{\partial \alpha}$, per radian

$C_{m_{\dot{\alpha}}} = \frac{\partial C_m}{\partial \frac{\dot{\alpha}\bar{c}}{2V}}$, per radian

$C_{m_q} = \frac{\partial C_m}{\partial \frac{\dot{\theta}\bar{c}}{2V}}$, per radian

D differential operator, $\frac{d}{dt}$ $\left(\frac{1}{D}\right.$ implies integration$\left.\right)$

σ angle between interceptor X body axis and radar line of sight, positive when line of sight is above body axis, radians unless otherwise specified

$\bar{R}$ distance from interceptor to target along line of sight, measured positive from interceptor to target, ft

Ω angular velocity of line of sight, $(\Omega = \dot{\sigma} + \dot{\theta})$, radians/sec; positive when line of sight is rotating upward

t_G time of flight of interceptor from instantaneous position to firing point, sec

τ time of flight of interceptor's rockets from firing point to predicted point of contact with target, sec

$\bar{M}$ predicted miss distance, measured positive from interceptor to target, ft

M_{LS} component of $\bar{M}$ along the instantaneous radar line of sight, positive when target is ahead of rockets at predicted time of impact, ft

M_{NLS} component of $\bar{M}$ perpendicular to the instantaneous radar line of sight, positive when target is below rockets at predicted time of impact, ft

ϵ_γ error in interceptor's flight path at any given instant,

$$\epsilon_\gamma \approx \frac{-M_{NLS}}{V_I t_G + \left(V_I + V_R\right)\tau}$$

τ_s elevator servo-system time constant, sec

ϵ_f output of filter, radians

τ_f filter time constant, sec

K steering-error gain, $\frac{\text{Radians/sec}}{\text{Radian}}$ or $\frac{\Delta n}{\text{Radian}}$

K_1 steering-error integration gain, $\frac{\text{Radians/sec}}{\text{Radians-sec}}$ or $\frac{\Delta n}{\text{Radians-sec}}$

K_2 steering-error differentiation gain, $\frac{\text{Radians/sec}}{\text{Radians/sec}}$ or $\frac{\Delta n}{\text{Radians/sec}}$

K_3 normal-acceleration error gain, $\frac{\text{Radians/sec}}{\text{Number of } g}$

K_4 normal-acceleration error integration gain, $\frac{\text{Radians/sec}}{\text{Number of } g}$

K_r pitch-rate gain, $\frac{\text{Radians/sec}}{\text{Radians/sec}}$

K_s elevator-servo gain constant, $\frac{\text{Radians}}{\text{Radians/sec}}$

τ_d ratio of steering-error differentiation gain to steering error gain $\frac{K_2}{K}$, sec

Subscripts:

I interceptor

R rocket

T target

L limit

ss steady state

i input

o initial value

A dot over a quantity indicates differentiation with respect to time. A bar over a quantity indicates a vector.

DISCUSSION OF GUIDANCE EQUATIONS, LONGITUDINAL CONTROL SYSTEM, AND INTERCEPTOR EQUATIONS OF MOTION

Guidance equations.- The longitudinal tracking problem against a target maneuvering with a constant normal acceleration $V_T\dot{\gamma}_T$ is shown diagrammatically in figure 1 for a lead collision type of navigation. For this type of navigation the interceptor endeavors to fly a straight-line path such that at only one point on the path the rockets may be fired and a hit obtained on the target. The vector equation relating the distances travelled by interceptor, rockets, and target in the time interval $(t_G + \tau)$, subsequent to any given instant, to the predicted miss distance is:

$$\bar{R} + \overline{2 \frac{V_T}{\dot{\gamma}_T} \sin \dot{\gamma}_T \frac{(t_G + \tau)}{2}} = \overline{V_I t_G} + \overline{\left(V_I + V_R\right)\tau} + \bar{M} \tag{1}$$

where $\bar{R}$ is the range vector from the interceptor, which is flying with the velocity V_I, to the target, which is flying with the velocity V_T. The parameter $\dot{\gamma}_T$ is the time rate of change of the target flight path, and $V_T/\dot{\gamma}_T$ is the radius of curvature of the target flight path. The time of flight from the given instant to the point at which the rockets are released is t_G, and τ is the time of flight of the rockets from the firing point to the predicted point of contact of the rockets with the target. For this investigation $\tau = 1.5$ seconds. The average rocket velocity, due to its own thrust, over the time τ is V_R. The distance between the rockets and target at the predicted time of impact is the miss distance vector $\bar{M}$. The components of equation (1) along and perpendicular to the instantaneous line of sight are:

$$\left.\begin{aligned}
&R + 2 \frac{V_T}{\dot{\gamma}_T} \sin \dot{\gamma}_T \frac{(t_G + \tau)}{2} \cos\left[\sigma + \theta - \gamma_T - \dot{\gamma}_T \frac{(t_G + \tau)}{2}\right] = \\
&\left[V_I t_G + \left(V_I + V_R\right)\tau\right]\cos(\sigma + \alpha) + M_{LS} \\
&2 \frac{V_T}{\dot{\gamma}_T} \sin \dot{\gamma}_T \frac{(t_G + \tau)}{2} \sin\left[\sigma + \theta - \gamma_T - \dot{\gamma}_T \frac{(t_G + \tau)}{2}\right] = \\
&\left[V_I t_G + \left(V_I + V_R\right)\tau\right]\sin(\sigma + \alpha) + M_{NLS}
\end{aligned}\right\} \tag{2}$$

For the assumption that

$$\cos \dot{\gamma}_T \frac{(t_G + \tau)}{2} \approx 1$$

and

$$\sin \dot{\gamma}_T \frac{(t_G + \tau)}{2} \approx \frac{\dot{\gamma}_T (t_G + \tau)}{2}$$

these equations become:

$$\left.\begin{aligned} &R + V_T(t_G + \tau) \cos(\sigma + \theta - \gamma_T) + \frac{1}{2} V_T\dot{\gamma}_T(t_G + \tau)^2 \sin(\sigma + \theta - \gamma_T) = \\ &V_I(t_G + \tau) \cos(\sigma + \alpha) + V_R\tau \cos(\sigma + \alpha) + M_{LS} \\ &V_T(t_G + \tau) \sin(\sigma + \theta - \gamma_T) - \frac{1}{2} V_T\dot{\gamma}_T(t_G + \tau)^2 \cos(\sigma + \theta - \gamma_T) = \\ &V_I(t_G + \tau) \sin(\sigma + \alpha) + V_R\tau \sin(\sigma + \alpha) + M_{NLS} \end{aligned}\right\} \quad (3)$$

This assumption essentially means that the components of the target normal acceleration along and perpendicular to the instantaneous radar line of sight are nearly constant over the time interval $(t_G + \tau)$. Equations (3) rewritten in terms of range rate $\dot{R}$ and line of sight rotation Ω are

$$\left.\begin{aligned} &R + \dot{R}(t_G + \tau) - V_R\tau \cos(\sigma + \alpha) + \frac{1}{2} V_T\dot{\gamma}_T(t_G + \tau)^2 \sin(\sigma + \theta - \gamma_T) = M_{LS} \\ &-R\Omega(t_G + \tau) - V_R\tau \sin(\sigma + \alpha) - \frac{1}{2} V_T\dot{\gamma}_T(t_G + \tau)^2 \cos(\sigma + \theta - \gamma_T) = M_{NLS} \end{aligned}\right\} \quad (4)$$

where

$$\dot{R} = V_T \cos(\sigma + \theta - \gamma_T) - V_I \cos(\sigma + \alpha)$$

$$-R\Omega = V_T \sin(\sigma + \theta - \gamma_T) - V_I \sin(\sigma + \alpha)$$

The target flight-path angle γ_T is taken as zero when the target is in level flight going away from the interceptor, and as π when in level flight coming toward the interceptor. For $\gamma_T < \pi/2$, a positive value of $\dot{\gamma}_T$ indicates a pitch-up of the target flight path, and for $\gamma_T > \pi/2$, a negative value of $\dot{\gamma}_T$ indicates a pitch-up. For the runs in this paper the initial flight-path angle of the target is taken as π (target coming toward interceptor).

In reference 1, the tie-in between the guidance and the longitudinal control system was accomplished by computing continuously the value of $(t_G + \tau)$ necessary for M_{LS} to be zero, and for these values of $(t_G + \tau)$, computing the predicted value of M_{NLS}. The command to the control system was based on the error ϵ_γ which exists at any time in the interceptor's flight path, and is approximated by

$$\epsilon_\gamma \approx \frac{-M_{NLS}}{V_I t_G + (V_I + V_R)\tau} \tag{5}$$

The time at which t_G is computed to be zero is taken as the firing time for the interceptor's rockets. Examination of equations (4) indicates that it is necessary to know the target flight-path angle γ_T and target normal acceleration $V_T\dot{\gamma}_T$ in order to solve these equations for $(t_G + \tau)$ and M_{NLS}. In order to evaluate the acceleration terms of equations (4) in a guidance computer, knowledge of derivatives of $\bar{R}$ of higher order than $\dot{\bar{R}}$ is required. Guidance systems of the type from which these derivatives would be available are difficult to mechanize, and are not being used. In view of this condition the target acceleration terms in equations (4) will be omitted, and the primary effect of the maneuvering target is assumed to be reflected in the parameters $\dot{R}$ and $R\Omega$ through changes in the target flight-path angle γ_T. When the acceleration terms are omitted, equations (4) become the first-order guidance equations presented in reference 1 for a nonmaneuvering target. It is apparent from examination of equations (4) that the $V_T\dot{\gamma}_T$ term can have only a negligible effect on the computed value of $(t_G + \tau)$, and can result in a maximum error of 36 feet in M_{NLS} for $V_T\dot{\gamma}_T = 32$ ft/sec^2 and $\tau = 1.5$ seconds, which are the values assumed in this investigation.

One of the most significant characteristics of this first order guidance is that the interceptor must maintain, in the steady state, a normal acceleration proportional to that of the target in order to carry out the tracking assignment against a target maneuvering with a constant normal acceleration. For the pitch-rate command system used for longitudinal control in reference 1, an error in the interceptor flight-path angle is required to command a steady interceptor normal acceleration, and hence this system is unable to track a maneuvering target with a zero error. The miss distance M_{NLS} associated with this required flight-path error will henceforth be referred to as the bias error. The introduction of a slow integration in the tracking loop should permit tracking with a zero bias error. Another possibility is to use a high static sensitivity between the interceptor normal acceleration and the interceptor flight-path error angle, which should minimize the bias error. However, both conditions should be investigated with respect to stability and performance against nonmaneuvering and maneuvering targets.

Control systems considered.- The automatic control systems considered in this investigation for controlling the interceptor's flight path include the pitch-rate system discussed in reference 1, and a normal acceleration control system which will be discussed subsequently in this paper. Block diagrams for both systems are presented in figure 2. The dynamics of the filter and elevator servo are represented by first-order lag networks of the form $\frac{1}{1 + \tau_f D}$ and $\frac{1}{1 + \tau_s D}$, respectively. For this investigation $\tau_f = 0.60$ second and $\tau_s = 0.03$ second. The filter would be used in practice to filter the noise out of the error signal ϵ_γ. No consideration is given to noise in this investigation, but the assumed dynamics of the filter are included in the analysis. The error signal ϵ_γ, subsequent to being filtered, is passed through an amplifier, a differentiator, and an integrator. The result of these operations is taken as the command to either a pitch-rate control system or normal-acceleration system. In either system the interceptor normal acceleration may be limited by limiting the input to these systems to the desired value. For this investigation the inputs to the control system were limited to values such that the interceptor static acceleration response would not exceed +5g or -2g.

Interceptor equations of motion.- The longitudinal dynamics of the interceptor were represented in this investigation by the following equations of motion, referred to wind axes:

$$\left.\begin{aligned}
&\frac{mV_{I_o}}{q_o S}\dot{\gamma} = \left(C_{L_\alpha}\Delta\alpha + C_{L_{\delta_e}}\delta_e\right)(1 + u') + 2C_{L_o}u' + \frac{W \sin \gamma_o}{q_o(1 + u')S}(\Delta\theta - \Delta\alpha) \\
&-\frac{mV_{I_o}}{q_o S}\dot{u}' = \Delta C_D + 2C_D u' + \frac{W \cos \gamma_o}{q_o S}(\Delta\theta - \Delta\alpha) \\
&\frac{I_Y}{q_o S\bar{c}}\ddot{\theta} = \left(C_{m_q}\frac{\bar{c}}{2V_{I_o}}\dot{\theta} + C_{m_{\dot{\alpha}}}\frac{\bar{c}}{2V_{I_o}}\dot{\alpha} + C_{m_\alpha}\Delta\alpha + C_{m_{\delta_e}}\delta_e\right)(1 + 2u')
\end{aligned}\right\} \qquad (6)$$

From unpublished wind-tunnel tests made for a model similar to the interceptor discussed in this paper, the variation of drag coefficient C_D in the vicinity of the interceptor's trim angle of attack and initial Mach number was found to be well approximated by

$$C_D = C_{D_o} + \Delta C_D$$

$$= 0.027 + 0.156\ \Delta\alpha + 2.37\ \Delta\alpha^2 - (0.013 + 0.134\ \Delta\alpha + 2.03\ \Delta\alpha^2)u'$$

and the variation of C_{L_α} with Mach number in this range was given by

$$C_{L_\alpha} = \frac{5.05}{M_o(1 + u')} = \frac{2.29}{1 + u'}$$

The interceptor stability derivatives, mass characteristics, and other constants used in this investigation are presented in table I. A detailed derivation of equations (6) is presented in appendix A, and the assumptions made are discussed.

RESULTS AND DISCUSSION

In the section entitled "Discussion of Guidance Equations, Longitudinal Control System, and Interceptor Equations of Motion" it was stated that an interceptor, which utilizes first-order guidance, must have a steady normal acceleration proportional to that of the target in order to track a target maneuvering with constant normal acceleration. Furthermore, for the longitudinal control systems discussed in this paper there must exist an error in the interceptor's flight path, with respect to that required for a hit, of sufficient magnitude to command this acceleration unless there is integration performed on the flight-path error. The magnitude of this bias error can be minimized by use of a high sensitivity between the interceptor's g-response and flight-path error if no integration is included. It may be necessary, however, to make additional modifications to the automatic-control system or tracking loop in order to insure adequate stability when high gains are used.

Control Systems

Pitch-rate command system.- The block diagram of the pitch-rate command system is shown in figure 2(a). In reference 1 good tracking performance against a nonmaneuvering target was calculated for this system for $K = 3.0$ and $K_r = 0.375$. For a maneuvering target, however, it can be shown that there will be a large bias error in the flight path, and hence miss distance, for this value of K. Since $(\Delta n)_{ss} = \frac{V}{g}\dot{\theta}_{ss}$, the following expression, which relates the interceptor steady normal acceleration to the value of M_{NLS} at the time of firing ($t_G = 0$), may be derived from the block diagram of figure 2 and equation (5):

$$\left(M_{NLS}\right)_{t_G=0} = \frac{-g\tau}{KV_{I_o}(1 + u')}\left[V_{I_o}(1 + u') + V_R\right]\left[\frac{1}{K_s}\left(\frac{\delta_e'}{\dot{\theta}}\right)_{ss} + K_r\right]\Delta n_{ss} \tag{7}$$

For

$$\tau = 1.5$$

$$V_I + V_R = 4,140$$

$$\frac{g}{V_{I_o}} = 0.015$$

$$K_r = 0.375$$

$$K_s = 1$$

$$\left(\frac{\delta_e'}{\dot{\theta}}\right)_{ss} = 4.85 \text{ (based on two degrees of freedom)}$$

$$(\Delta n)_{ss} \approx \Delta n_T = 1$$

and if $u' = 0$

$$\left(M_{NLS}\right)_{t_G=0} = \frac{-487}{K}$$

Therefore, for M_{NLS} to be less than 50 feet, when $t_G = 0$, for this assumed case K must be approximately 10 or greater. For $K = 3.0$, which was used in reference 1 for the nonmaneuvering target, M_{NLS} would be approximately -160 feet for this target acceleration. For a practical case in which the interceptor speed would decrease, gains even larger would be required.

System response without integration in tracking loop: Results are presented in figure 3 which afford a comparison of the interceptor's attack performance against a nonmaneuvering target and against one maneuvering with 1g normal acceleration when no integrator is in the tracking loop. The runs shown in figure 3(a) are for control system gains which give a reasonable response for the case of a nonmaneuvering target. For these runs $R_o = 60{,}000$ feet, $\sigma_o = 7.5^o$, $\gamma_{I_o} = 0$, and $\gamma_{T_o} = \pi$. For these and subsequent runs the transient responses are plotted up to the assumed time of rocket firing ($t_G = 0$). For comparison, lines of constant flight-path error of 20 mils are shown. These lines are shown only in this figure but are the same for all the runs presented. It is apparent that for $\Delta n_T = 1$, the predicted value of M_{NLS} is about -300 feet when the rockets are fired ($t_G = 0$). The value of M_{NLS} at $t_G = 0$ predicted by equation (7) for $(\Delta n)_{ss}$ and u'_{ss} shown on figure 3(a) is about -260 feet, as compared to the value of -300 feet indicated by the REAC calculations. There is a small bias error attributable to the interceptor's loss in forward speed which can be seen from the results for the nonmaneuvering case. As the interceptor loses speed, a continuous error is generated in the flight-path angle and, probably more important, a change in the trim angle of attack occurs as the interceptor speed is reduced. This bias can be eliminated, or at least markedly reduced, by introduction of a signal to the elevator servo proportional to the loss in forward speed, which corrects for the out-of-trim pitching moment due to the loss in speed. Results for the case where this feedback is added are also presented in figure 3(a). This bias due to u' could also be eliminated by use of an integration between ϵ_γ and δ_e, or minimized by use of a high gain between these quantities. The responses presented in figure 3(b) are for a set of control-system gains which were about the best found for the maneuvering target case. The responses for both target conditions are seen to be very oscillatory for this high gain and no improvement was obtained from further increases in K_r.

System responses with integration in tracking loop: Results are presented in figures 4(a) and 4(b) which show the effect of integration in the tracking loop on the system responses against maneuvering and nonmaneuvering targets. The effect of the integrator is to eliminate the bias error against the maneuvering target (fig. 4(a)), but the integration causes a large overshoot in the miss distance for the nonmaneuvering target case (fig. 4(b)). Another disadvantage of the integrator can be seen from figure 5. Responses are shown for various initial lock-on errors, and although the responses are good for $\sigma_o = 7.5^o$, the integral gain used is too large for $\sigma_o = 10^o$ and too small for $\sigma_o = 2^o$. It appears that if an integrator is used it may be necessary to use an integrator gain which is a function of lock-on error, or some similar nonlinear arrangement, in order to get satisfactory responses over the range of σ_o likely to be encountered. It should be pointed out that, when a high gain is used between $\dot{\theta}_i$ and ϵ_γ instead of the integration, the quality of the system responses are essentially independent of σ_o.

Effect of high gain plus differentiation in tracking loop: The high gain cases presented in figure 3(b) were seen to be very oscillatory and hence undesirable. This condition could be improved by the use of differentiation in the tracking loop to provide flight-path stabilization. The equation for $\dot{\theta}_i$ would then become

$$\dot{\theta}_i = K\epsilon_f + K_2\dot{\epsilon}_f$$

Results are presented in figures 6(a) and 6(b) for maneuvering and nonmaneuvering targets which show the effect of the differentiation gain K_2 on the system responses. There is a large increase in tracking loop damping as K_2 is introduced. Although K_2 tends to stabilize the tracking loop, it tends to reduce the effectiveness of the filter, and hence might not be acceptable from the standpoint of system noise. This can be seen by considering the transfer function $\frac{\dot{\theta}_i}{\epsilon_\gamma}$ which is

$$\frac{\dot{\theta}_i}{\epsilon_\gamma} = \frac{K(1 + \tau_d D)}{(1 + \tau_f D)}$$

where

$$\tau_d = \frac{K_2}{K}$$

Therefore, the introduction of differentiation in the tracking loop is somewhat comparable to reducing the filter time constant. For example, when $\tau_d = \tau_f$, the filtering is completely eliminated. It can be deduced from these results that this high-gain system could be made very stable provided that a filter time constant roughly 50 percent of the value assumed (0.60) would give acceptable filtering.

Normal-acceleration command system.- In the present investigation, the basic error involved is ϵ_γ, which is the instantaneous error in the interceptor's flight path. The interceptor normal acceleration is proportional to the rate of change of the flight path; hence, a system in which a normal acceleration is commanded proportional to the flight-path error appears to be a very logical type of longitudinal control system for the present problem. Control systems similar to this system are discussed in references 3 and 4. The block diagram of the normal-acceleration system is presented in figure 2. It should be noted that there is an integration in the normal-acceleration command loop. A signal equivalent to $\cos\theta$ is subtracted from the accelerometer output in order to zero the feedback signal to the elevator servo when no change is desired in the flight path of the interceptor. Subtraction of this quantity effectively converts the accelerometer output to a Δn or $\dot{\gamma}_I$ feedback.

System response without integration in tracking loop ($K_1 = 0$): Results are presented in figure 7 for nonmaneuvering and maneuvering target conditions for two values of steering-error gain K. The results shown in figure 7(a) are for $K = 33.0$, which gives a good response for the nonmaneuvering target, but there is seen to be a large bias error in the miss distance for this gain for the maneuvering target case. It will be noted that there is no bias due to u' for the nonmaneuvering case for this control system such as that computed for the pitch-rate system. This bias is eliminated by the self-trimming properties of the normal-acceleration system which are provided by the integrator in the normal-acceleration command loop. The responses shown in figure 7(b) are for $K = 200.0$. The responses for both target conditions are oscillatory but the bias error for the maneuvering target case is reduced to a fairly low level at the assumed firing point. For this high value of K it was necessary to reduce the gain of the integrator in the control loop to zero in order to keep the overall system stable. This removes the self-trimming properties of the system, but the bias error due to change in trim is very small since the static gain between ϵ_γ and δ_e is $K\left(K_3\right) = 42.0$ for this case.

System responses with integrator in tracking loop: The effects of integration in the tracking loop on the system responses are seen in figures 8(a) and 8(b). The same trends are noted for this normal-acceleration system as were noted for the pitch-rate system. The responses for the maneuvering target case for $\sigma_o = 7.5^\circ$ with $K = 33.0$ and $K_1 = 0.93$ (fig. 8(a)) indicate that the bias error is eliminated by the integration, but for the nonmaneuvering target condition (fig. 8(b)) there is a large overshoot in the M_{NLS} transient. Although results are not presented for values of σ_o other than 7.5°, the same dependence of the motions on lock-on error exists for this system as for the pitch-rate system discussed previously.

System responses with high gain plus lead in tracking loop: Results are presented in figures 9(a) and 9(b) which show the effect on the system stability of incorporating lead or differentiation in the tracking loop, and the results shown for this control system are similar to those obtained for the pitch-rate system. The differentiation in the tracking loop has a large stabilizing effect on the system responses, but as mentioned previously, it might not be desirable from the standpoint of system noise.

Effect of Limiting Rate of Control Deflection

The responses presented up to this point were computed for the assumption that $(\dot{\delta}_e)_{max} = \pm 120^{\circ}/\text{sec}$ and $(\delta_e)_{max} = \pm 20^{\circ}$. In order to investigate the effects of reducing the maximum available control rate, calculations were made for $(\dot{\delta}_e)_{max} = 80^{\circ}/\text{sec}$ and $60^{\circ}/\text{sec}$ and the results are presented in figures 10(a) and 10(b) for two values of pitch-rate gain K_r. The results are for the normal-acceleration control system, and are for high gain only in the tracking loop. For $K_r = 1$, the system is seen to be unstable for $(\dot{\delta}_e)_{max} = 60^{\circ}/\text{sec}$. However, for $K_r = 2.0$ (fig. 10(b)), this instability is not present. This comparison indicates that pitch-rate feedback can be used to eliminate instability caused by low available control rates. The results presented in figure 10(c) demonstrate another means of eliminating instability caused by low available control rates. For this run, $(\dot{\delta}_e)_{max} = 60^{\circ}/\text{sec}$ and a feedback to the servo proportional to pitching acceleration has been assumed. This feedback is seen to have a very stabilizing effect on the condition shown. The runs presented in figure 10 for $K_r = 2.0$ were repeated for the case where the steering-error differentiation was included in the tracking loop, and the results are shown in figures 10(d) and 10(e) for $K_2 = 120$. It can be seen from figure 10(d) that inclusion of lead resulted in instability for $(\dot{\delta}_e)_{max} = 60^{\circ}/\text{sec}$, whereas for $K_2 = 0$ (fig. 10(b)), the system was stable for this control rate. However, inclusion of pitch acceleration feedback (fig. 10(e)) is seen to eliminate this instability.

CONCLUSIONS

From the results presented in this paper the following conclusions can be drawn:

1. For the control systems considered, a bias error will exist in the flight path of an interceptor which utilizes a first-order guidance computer that must accelerate in the steady state when tracking a target which is maneuvering with a constant normal acceleration, unless an integration is performed on the flight-path error.

2. The effect of integration in the tracking loop is to cause large overshoots against nonmaneuvering targets and to give a system response against maneuvering targets which depends on the initial lock-on error and target accelerations.

3. Use of high tracking gain in lieu of integration tended to minimize the bias errors against maneuvering targets but the stability of the system responses, particularly those obtained when the pitch-rate command was utilized, was poor.

4. Inclusion of a signal proportional to the derivative of the filtered flight-path error as part of the command to the control system resulted in good tracking stability for both the pitch-rate and normal-acceleration systems. This type of signal, however, might be undesirable from other considerations such as system noise.

5. Bias errors in the flight path which result from an interceptor trim change during the attack run, can be eliminated by use of integration in the control loop, or minimized by use of a high gain between the flight-path error and the elevator deflection. Also, a feedback to the elevator servo proportional to change in forward speed was shown to be capable of eliminating or minimizing the bias errors due to trim changes.

6. Reductions in the available control-deflection rate were shown to have a destabilizing effect on the system responses, but this destabilizing effect could be counteracted by use of high pitch-rate feedback or by use of pitch-acceleration feedback.

Langley Aeronautical Laboratory,
National Advisory Committee for Aeronautics,
Langley Field, Va., July 15, 1955.

APPENDIX A

DERIVATION OF AIRFRAME LONGITUDINAL EQUATIONS USED IN INVESTIGATION

The airframe equations of longitudinal motion used in this paper are derived from the following general longitudinal equations which are referred to wind axes:

$$\left.\begin{aligned} mV\dot{\gamma} &= L - W\cos\gamma \\ m\dot{V} &= -D - W\sin\gamma + T \\ I_Y\ddot{\theta} &= M' \end{aligned}\right\} \tag{A1}$$

The thrust T is assumed to be aligned with the wind at all times. Substitution of

$$L = L_o + \Delta L$$

$$\gamma = \gamma_o + \Delta\gamma$$

$$T = T_o$$

$$V = V_o + \Delta V = V_o(1 + u')$$

$$D = D_o + \Delta D$$

$$M' = \Delta M'$$

$$L_o - W\cos\gamma_o = 0$$

$$-D_o - W\sin\gamma_o + T_o = 0$$

into equations (A1) yields the following equations, for the assumption that $\cos\Delta\gamma = 1$ and $\sin\Delta\gamma = \Delta\gamma$:

$$\left.\begin{aligned}
mV_o(1 + u')\dot{\gamma} &= \Delta L + \Delta\gamma W \sin \gamma_o \\
mV_o\dot{u}' &= -\Delta D - \Delta\gamma W \cos \gamma_o \\
I_y\ddot{\theta} &= \Delta M'
\end{aligned}\right\} \tag{A2}$$

The quantities ΔL, ΔD, and $\Delta M'$ may be obtained from the relations

$$\left(L_o + \Delta L\right) = \left(C_{L_o} + \Delta C_L\right)\left(q_o + \Delta q\right)S$$

$$\left(D_o + \Delta D\right) = \left(C_{D_o} + \Delta C_D\right)\left(q_o + \Delta q\right)S$$

$$\Delta M' = \Delta C_m\left(q_o + \Delta q\right)S\bar{c}$$

The expressions for these quantities are

$$\left.\begin{aligned}
\Delta L &= C_{L_o}\ \Delta qS + \Delta C_L q_o S + \Delta C_L\ \Delta qS \\
\Delta D &= C_{D_o}\ \Delta qS + \Delta C_D q_o S + \Delta C_D\ \Delta qS \\
\Delta M' &= \Delta C_m q_o S\bar{c} + \Delta C_m\ \Delta qS\bar{c}
\end{aligned}\right\} \tag{A3}$$

The quantities C_{L_o} and C_{D_o} are functions of the trim angle of attack α_o and the initial forward velocity V_o, and q_o is a function of V_o and the initial altitude of the interceptor. The quantity Δq is given by

$$\Delta q = q_o(2u' + \rho' + 2\rho'u' + u'^2 + \rho'u'^2) \tag{A4}$$

where

$$\rho' = \frac{\Delta\rho}{\rho_o}$$

and

$$u' = \frac{\Delta V}{V_o}$$

Substitution of equations (A3) into equations (A2) yields the following set of equations:

$$\left.\begin{aligned}
\frac{mV_o}{q_oS}(1 + u')\dot{\gamma} &= C_{L_o}\frac{\Delta q}{q_o} + \Delta C_L\left(1 + \frac{\Delta q}{q_o}\right) + \frac{W \sin \gamma_o}{q_oS}\Delta\gamma \\
-\frac{mV_o}{q_oS}\dot{u}' &= C_{D_o}\frac{\Delta q}{q_o} + \Delta C_D\left(1 + \frac{\Delta q}{q_o}\right) + \frac{W \cos \gamma_o}{q_oS}\Delta\gamma \\
\frac{I_Y}{q_oS\bar{c}}\ddot{\theta} &= \Delta C_m\left(1 + \frac{\Delta q}{q_o}\right)
\end{aligned}\right\} \tag{A5}$$

For the assumption of no change in density, equation (A4) becomes

$$\frac{\Delta q}{q_o} = 2u' + u'^2$$

Substitution of this expression into equations (A5) gives

$$\frac{mV_{I_o}\dot{\gamma}}{q_oS} = C_{L_o}\left(\frac{2u' + u'^2}{1 + u'}\right) + \Delta C_L(1 + u') + \frac{W \sin \gamma_o}{q_oS(1 + u')}\Delta\gamma$$

$$-\frac{mV_{I_o}\dot{u}'}{q_oS} = C_{D_o}(2u' + u'^2) + \Delta C_D(1 + 2u' + u'^2) + \frac{W \cos \gamma_o}{q_oS}\Delta\gamma$$

$$\frac{I_Y}{q_oS\bar{c}}\ddot{\theta} = \Delta C_m(1 + 2u' + u'^2)$$

which, when only first-order terms in u' are retained and for

$$\Delta C_L = C_{L_\alpha}\Delta\alpha + C_{L_{\delta_e}}\delta_e$$

$$\Delta C_m = C_{m_q}\frac{\bar{c}}{2V_{I_o}}\dot{\theta} + C_{m_{\dot{\alpha}}}\frac{\bar{c}}{2V_{I_o}}\dot{\alpha} + C_{m_\alpha}\Delta\alpha + C_{m_{\delta_e}}\delta_e$$

reduced to

$$\frac{mV_{I_o}}{q_oS}\,\dot{\gamma} = 2C_{L_o}u' + \left(C_{L_\alpha}\,\Delta\alpha + C_{L_{\delta_e}}\delta_e\right)(1 + u') + \frac{W \sin \gamma_o}{q_oS(1 + u')}\,\Delta\gamma$$

$$-\frac{mV_{I_o}}{q_oS}\,\dot{u}' = 2C_Du' + \Delta C_D + \frac{W \cos \gamma_o}{q_oS}\,\Delta\gamma$$

$$\frac{I_Y}{q_oS\bar{c}}\,\ddot{\theta} = \left(C_{m_q}\frac{\bar{c}}{2V_{I_o}}\,\dot{\theta} + C_{m_{\dot{\alpha}}}\frac{\bar{c}}{2V_{I_o}}\,\dot{\alpha} + C_{m_\alpha}\,\Delta\alpha + C_{m_{\delta_e}}\delta_e\right)(1 + 2u')$$

which are the equations presented as equations (6) of the report.

REFERENCES

1. Gates, Ordway B., Jr., and Woodling, C. H.: Theoretical Analysis of the Longitudinal Behavior of an Automatically Controlled Supersonic Interceptor During the Attack Phase. NACA RM L54K08, 1955.

2. Margolis, Kenneth, and Bobbitt, Percy J.: Theoretical Calculations of the Stability Derivatives at Supersonic Speeds for a High-Speed Airplane Configuration. NACA RM L53G17, 1953.

3. Seaberg, Ernest C., and Smith, Earl F.: Theoretical Investigation of an Automatic Control System With Primary Sensitivity to Normal Accelerations as Used To Control a Supersonic Canard Missile Configuration. NACA RM L51D23, 1951.

4. Stokes, Fred H., and Mathews, Charles W.: Theoretical Investigation of Longitudinal Response Characteristics of a Swept-Wing Fighter Airplane Having a Normal-Acceleration Control System and a Comparison With Other Types of Systems. NACA TN 3191, 1954.

TABLE I.- STABILITY DERIVATIVES AND MASS CHARACTERISTICS OF

INTERCEPTOR AND OTHER CONSTANTS USED IN INVESTIGATION

Altitude, ft	50,000
ρ, slugs/ft^3	0.0003622
V_{I_o}, ft/sec	2140 (M = 2.2)
m, slugs	776.4
I_Y, slugs-ft^2	2.68×10^5
q, lb/ft^2	826
$\bar{c}$, ft	15
S, sq ft	401
C_{m_q}, per radian	-2.84
C_{m_α}, per radian	-0.56
$C_{m_{\dot{\alpha}}}$, per radian	-0.28
$C_{m_{u'}}$, per radian	0.00
C_{L_α}, per radian	2.29
C_{D_α}, per radian	0.156
C_{D_o}	0.027
C_L	0.076
$C_{m_{\delta_e}}$, per radian	-0.295
$C_{L_{\delta_e}}$, per radian	0.165
V_R, ft/sec	2,000
V_T, ft/sec	1,360
τ_s, sec	0.03
τ_f, sec	0.60
τ, sec	1.5
R_o, ft	60,000
θ_o, radians	0.033
α_o, radians	0.033
K_s, radians/radian/sec	1.0
$\left(\frac{\delta_e'}{\dot{\theta}}\right)_{ss}$	4.85

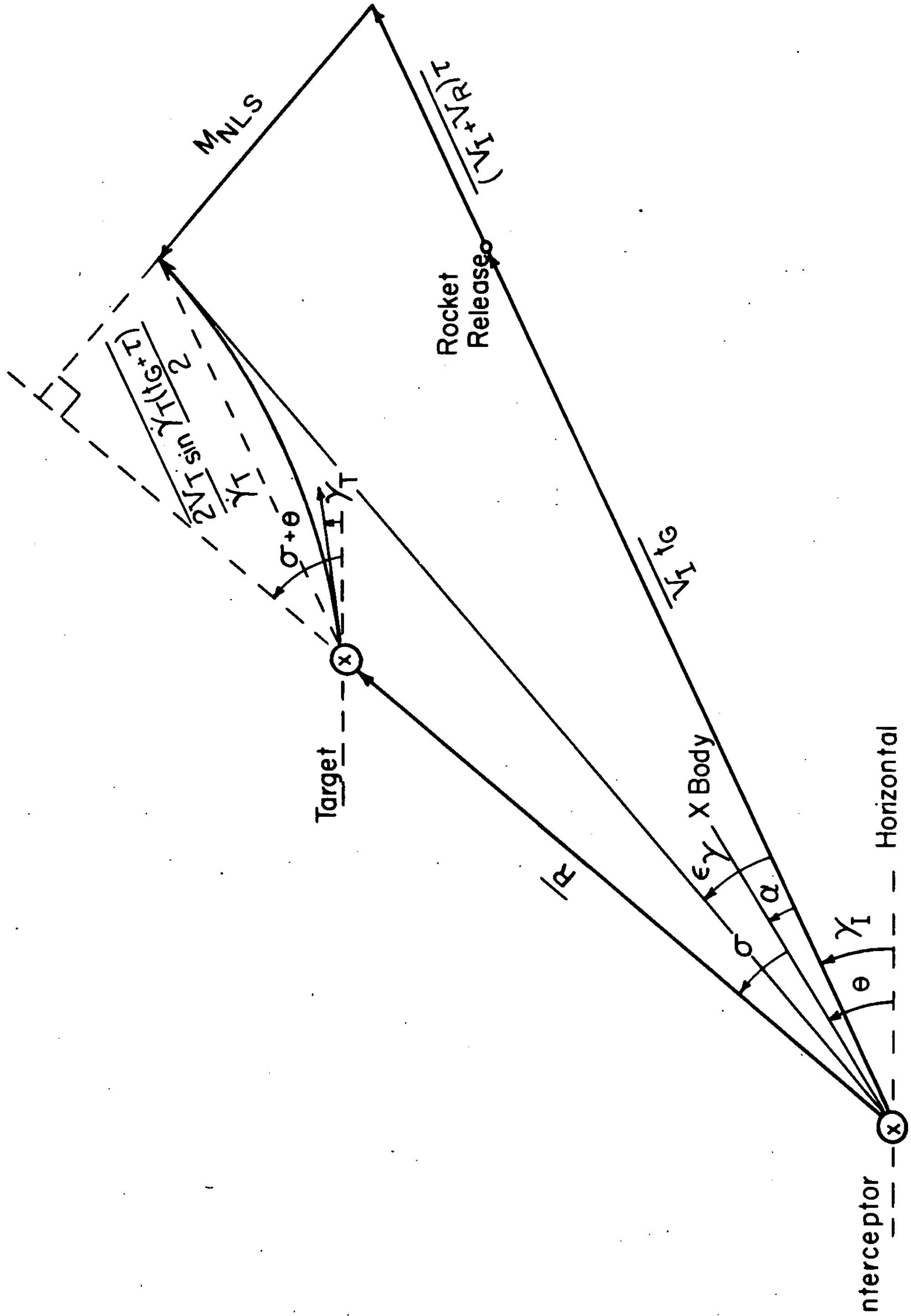

Figure 1.- Geometry of lead collision navigation for target performing constant-g pull-up. $M_{LS} = 0$; $\overline{M} = M_{NLS}$.

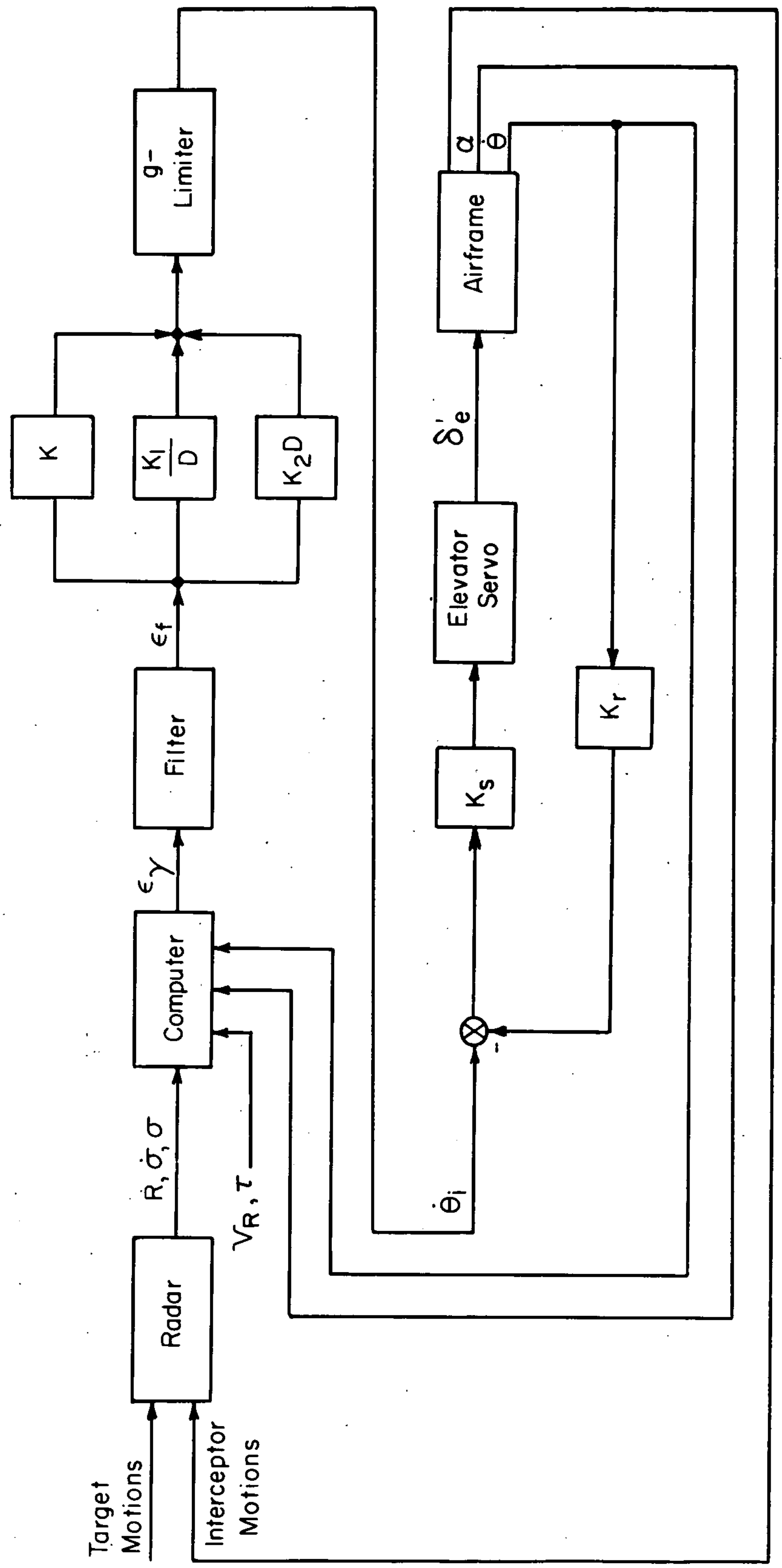

(a) Pitch-rate command system.

Figure 2.- Block diagrams of the longitudinal tracking systems used in present investigation.

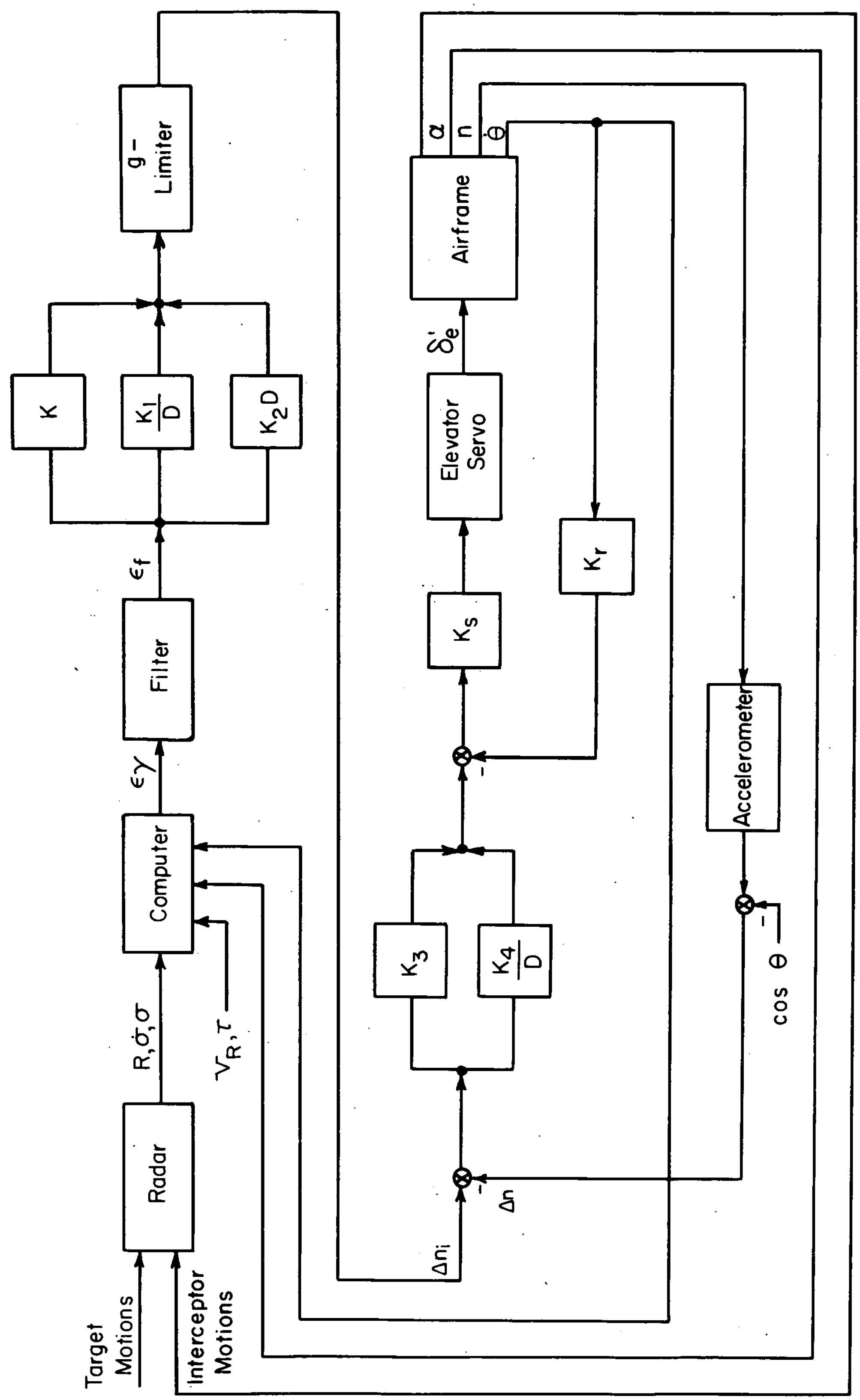

(b) Normal-acceleration command system.

Figure 2.- Concluded.

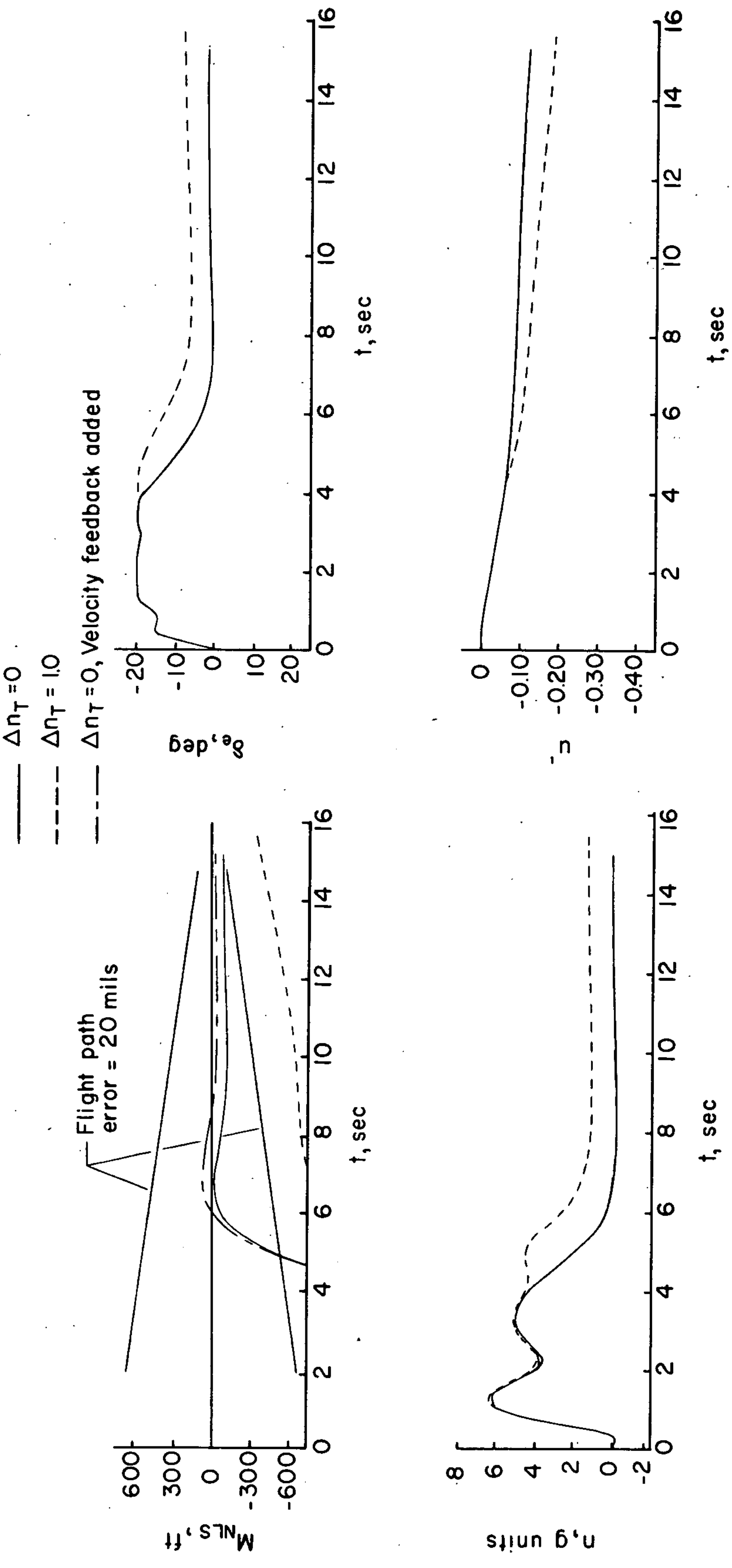

(a) $K = 3.0$; $K_r = 0.375$; $K_1 = K_2 = 0$.

Figure 3.- Interceptor and kinematic time histories. Pitch-rate command system; $R_o = 60{,}000$ ft; $\sigma_o = 7.5^\circ$; $\gamma_{I_o} = 0$; $\gamma_{T_o} = \pi$.

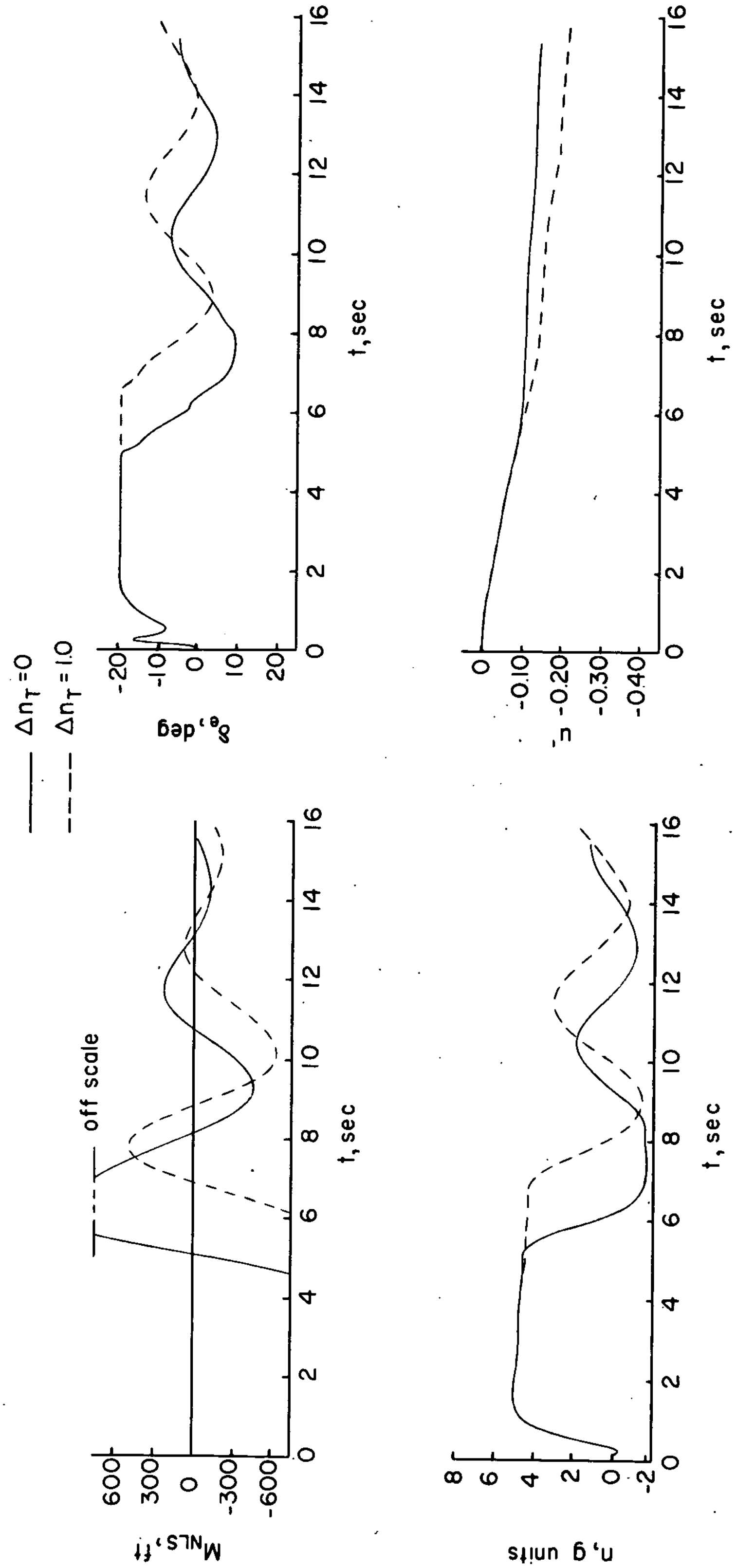

(b) $K = 9.0$; $K_r = 1.0$; $K_1 = K_2 = 0$.

Figure 3.- Concluded.

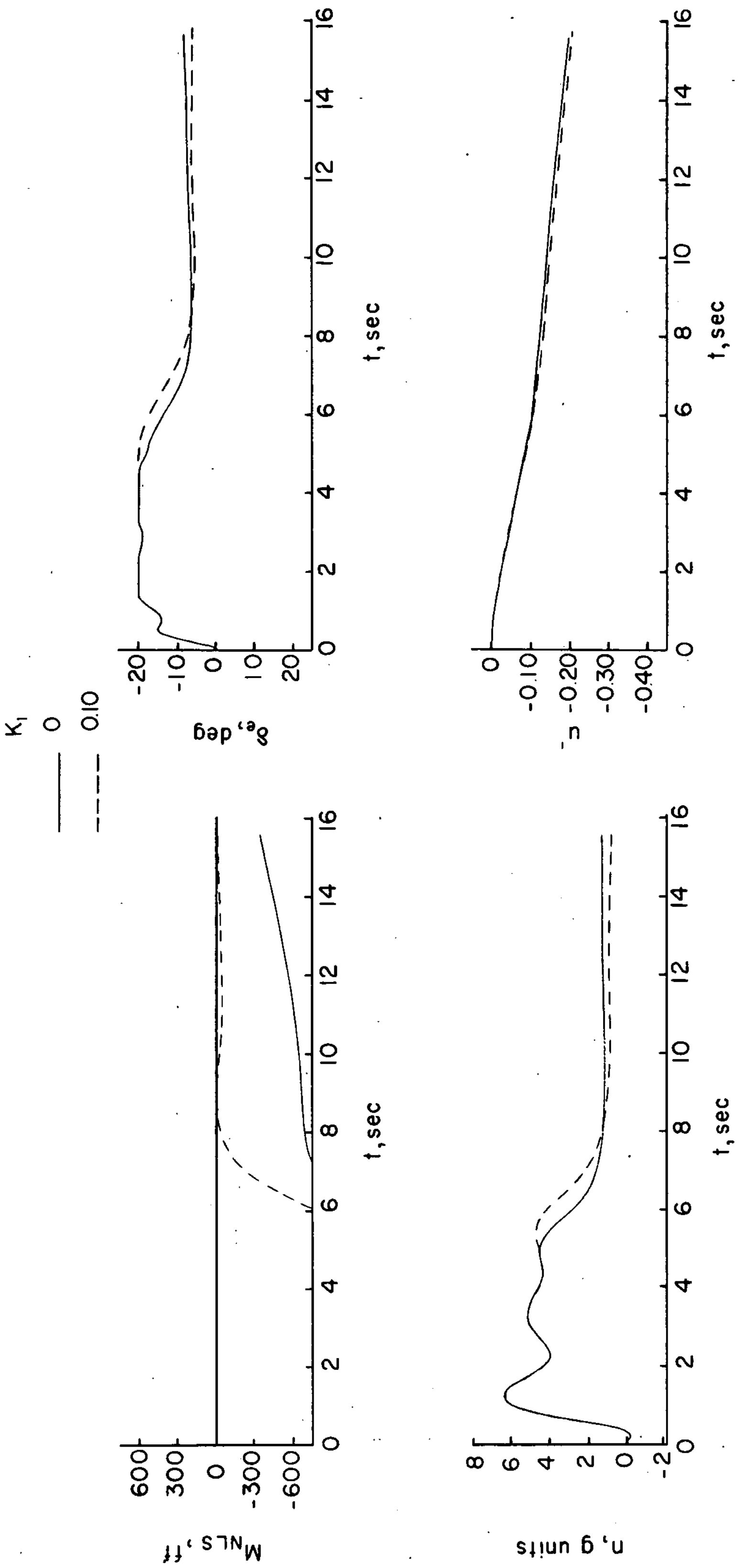

(a) $K = 3.0$; $K_r = 0.375$; $K_2 = 0$; $\Delta n_T = 1$.

Figure 4.- Effect of steering-error integration gain K_1 on interceptor attack performance. Pitch-rate command system; $R_o = 60,000$ ft; $\sigma_o = 7.5^o$; $\gamma_{I_o} = 0$; $\gamma_{T_o} = \pi$.

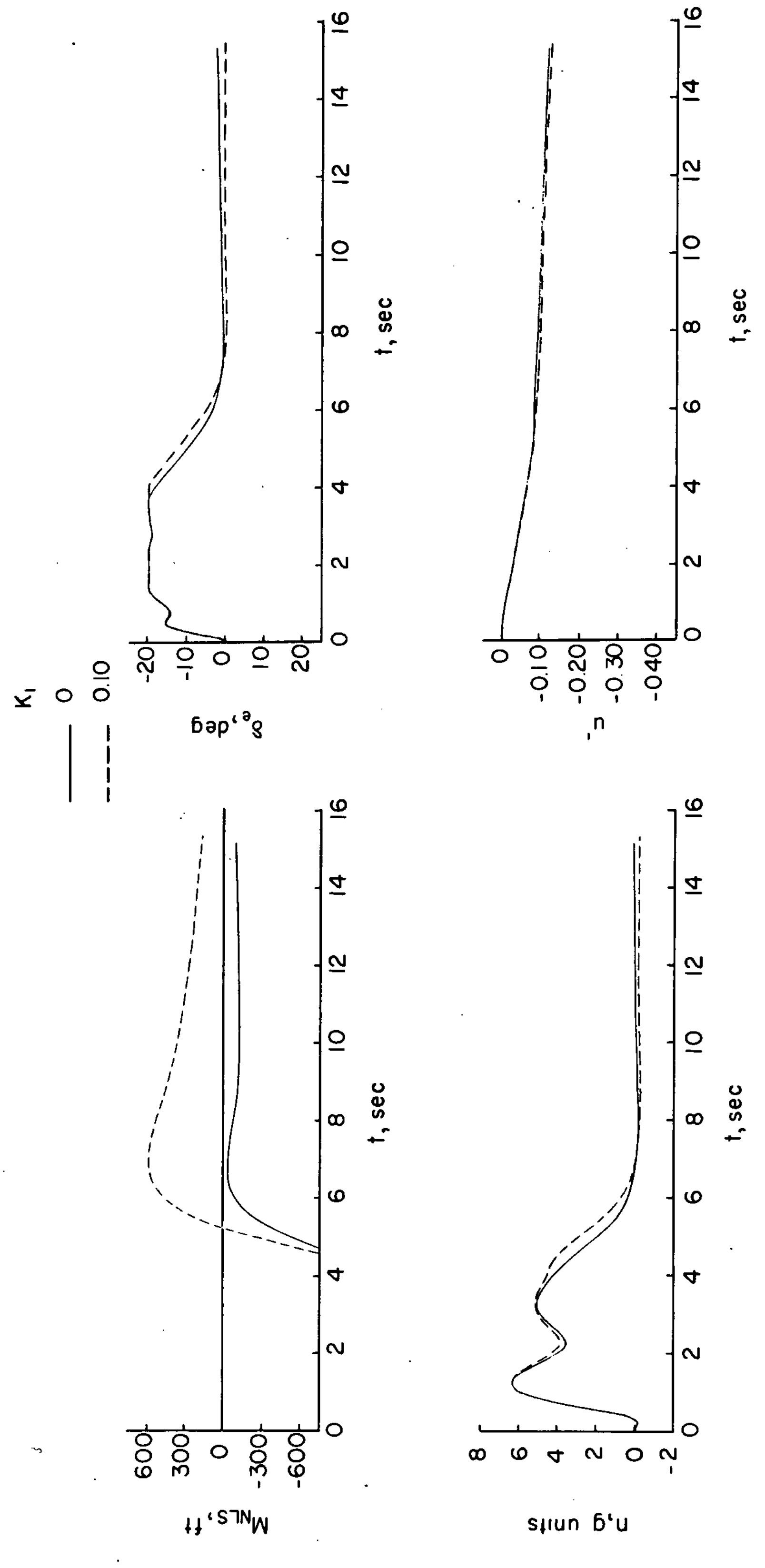

(b) $K = 3.0$; $K_r = 0.375$; $K_2 = 0$; $\Delta n_T = 0$.

Figure 4.- Concluded.

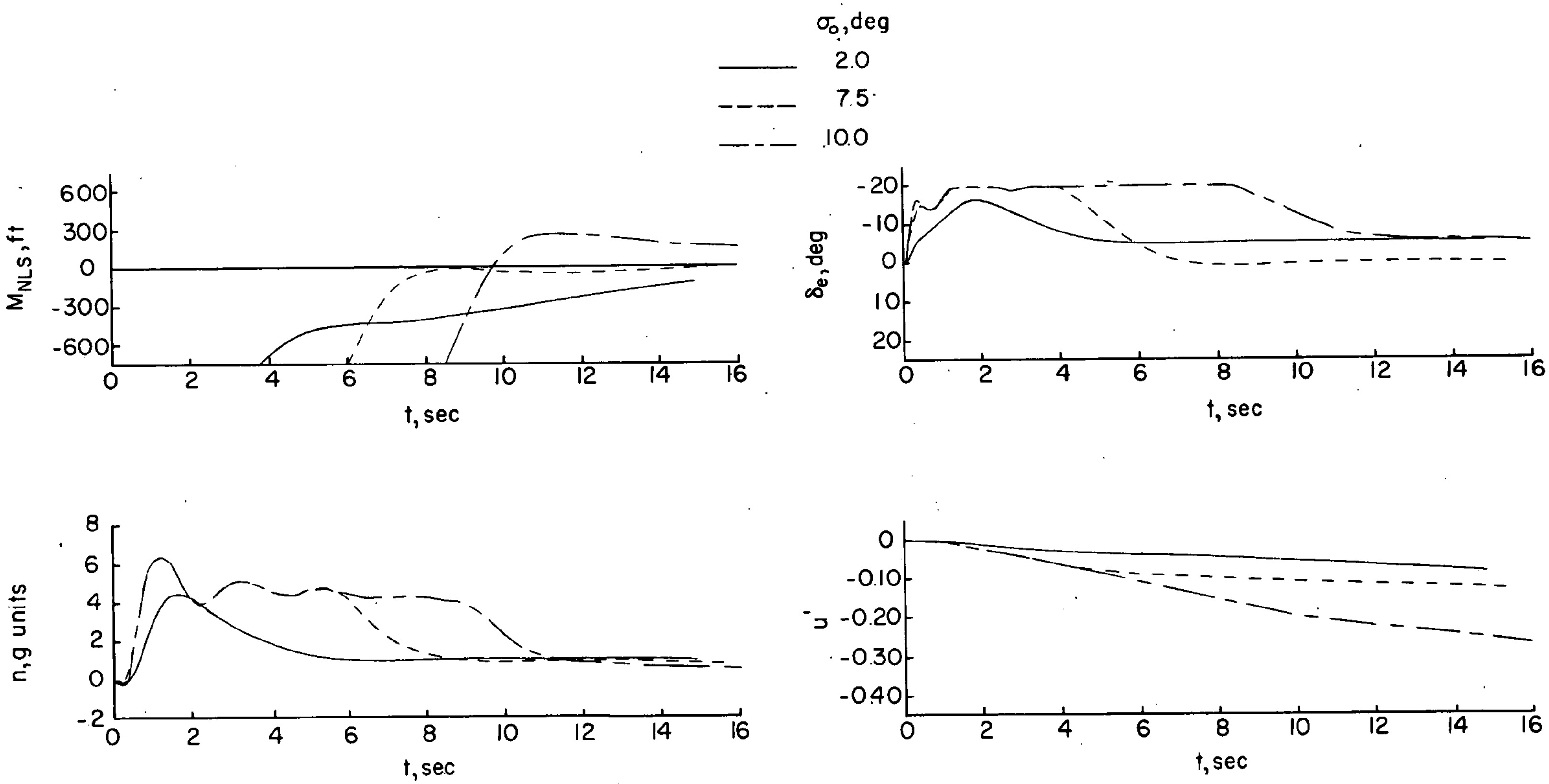

Figure 5.- Effect of initial values of radar elevation angle σ on interceptor attack performance with integration in tracking loop. Pitch-rate command system; R_o = 60,000 ft; K = 3.0; K_r = 0.375; K_1 = 0.10; K_2 = 0; Δn_T = 1; γ_{I_o} = 0; γ_{T_o} = π.

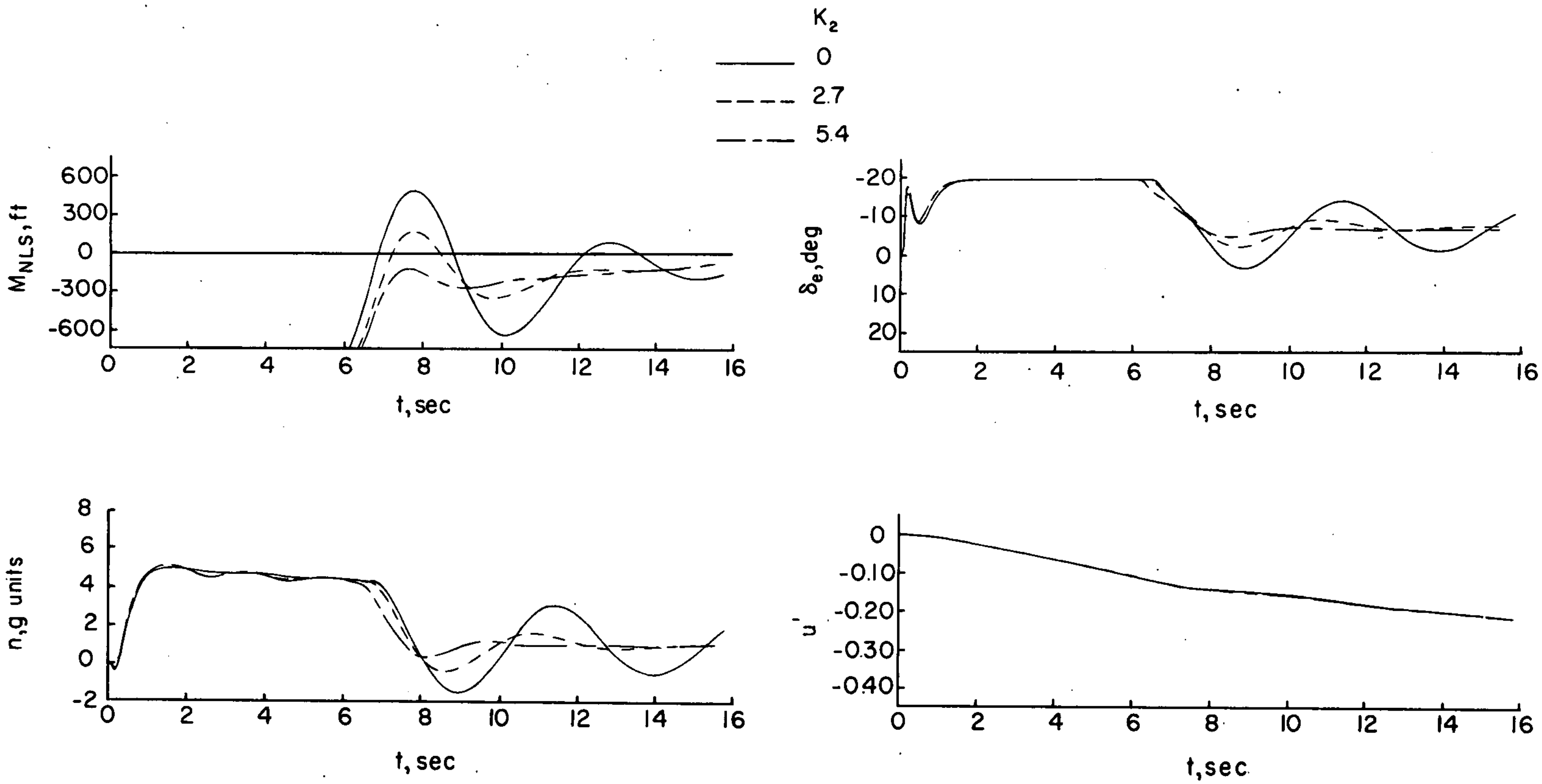

(a) $\Delta n_T = 1$.

Figure 6.- Effect of steering-error differentiation gain K_2 on interceptor attack performance. Pitch-rate command system; $R_o = 60,000$ ft; $\sigma_o = 7.5^o$; $K = 9.0$; $K_r = 1.0$; $K_1 = 0$; $\gamma_{I_o} = 0$; $\gamma_{T_o} = \pi$.

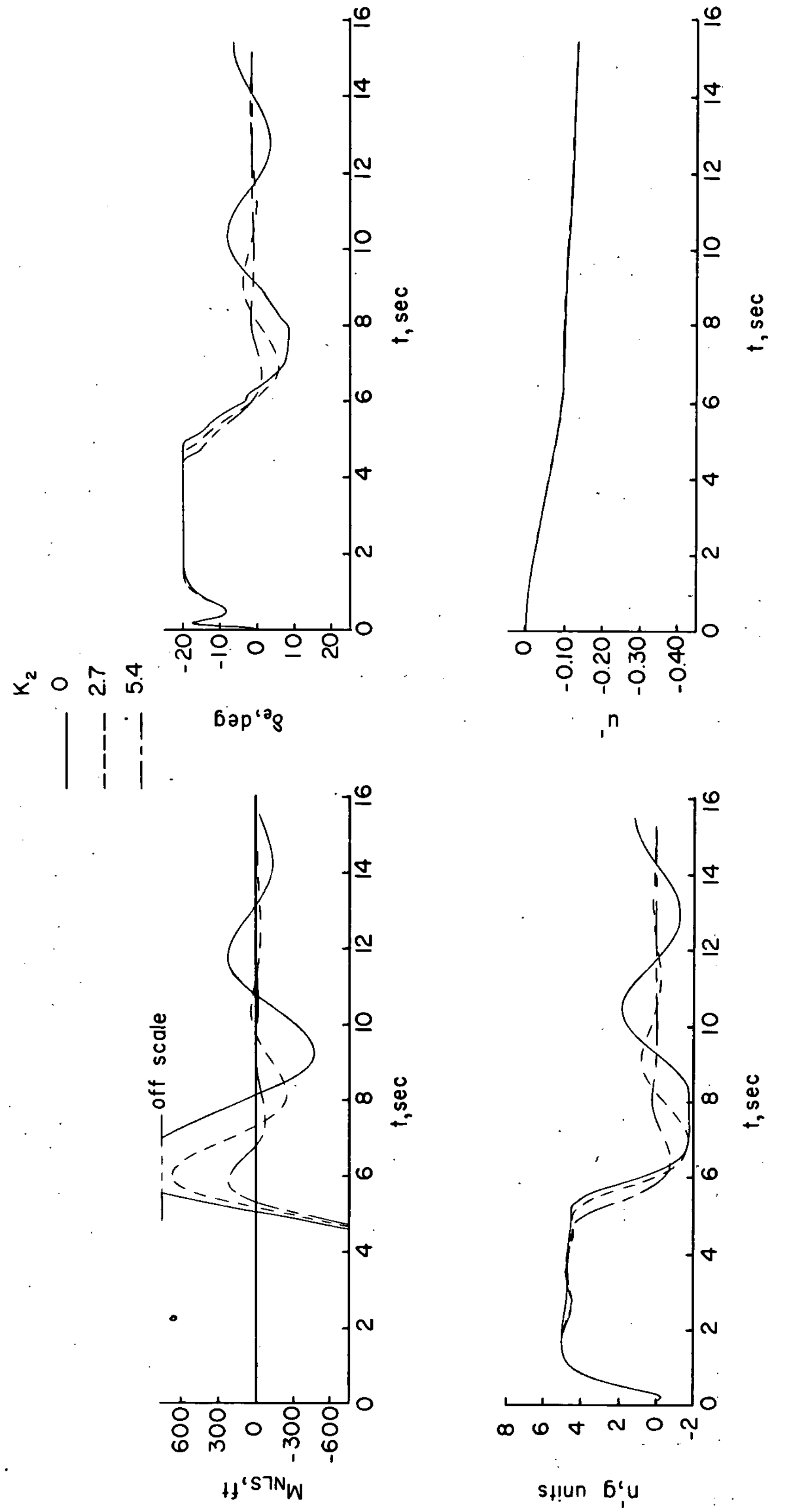

(b) $\Delta n_T = 0$.

Figure 6.- Concluded.

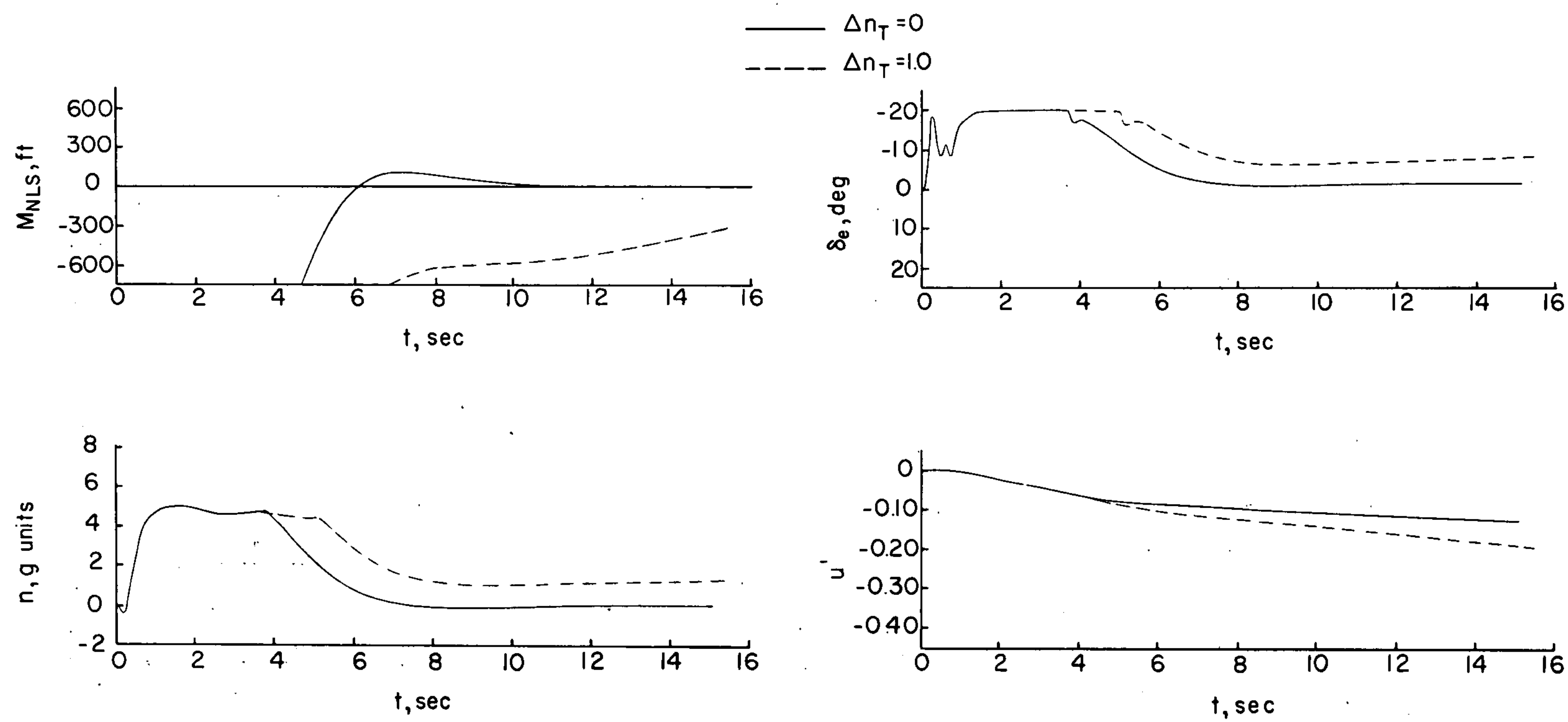

(a) $K = 33.0$; $K_1 = K_2 = 0$; $K_3 = 0.21$; $K_4 = 0.30$; $K_r = 2.0$.

Figure 7.- Interceptor and kinematic time histories. Normal-acceleration command system; $R_o = 60{,}000$ ft; $\sigma_o = 7.5^\circ$; $\gamma_{I_o} = 0$; $\gamma_{T_o} = \pi$.

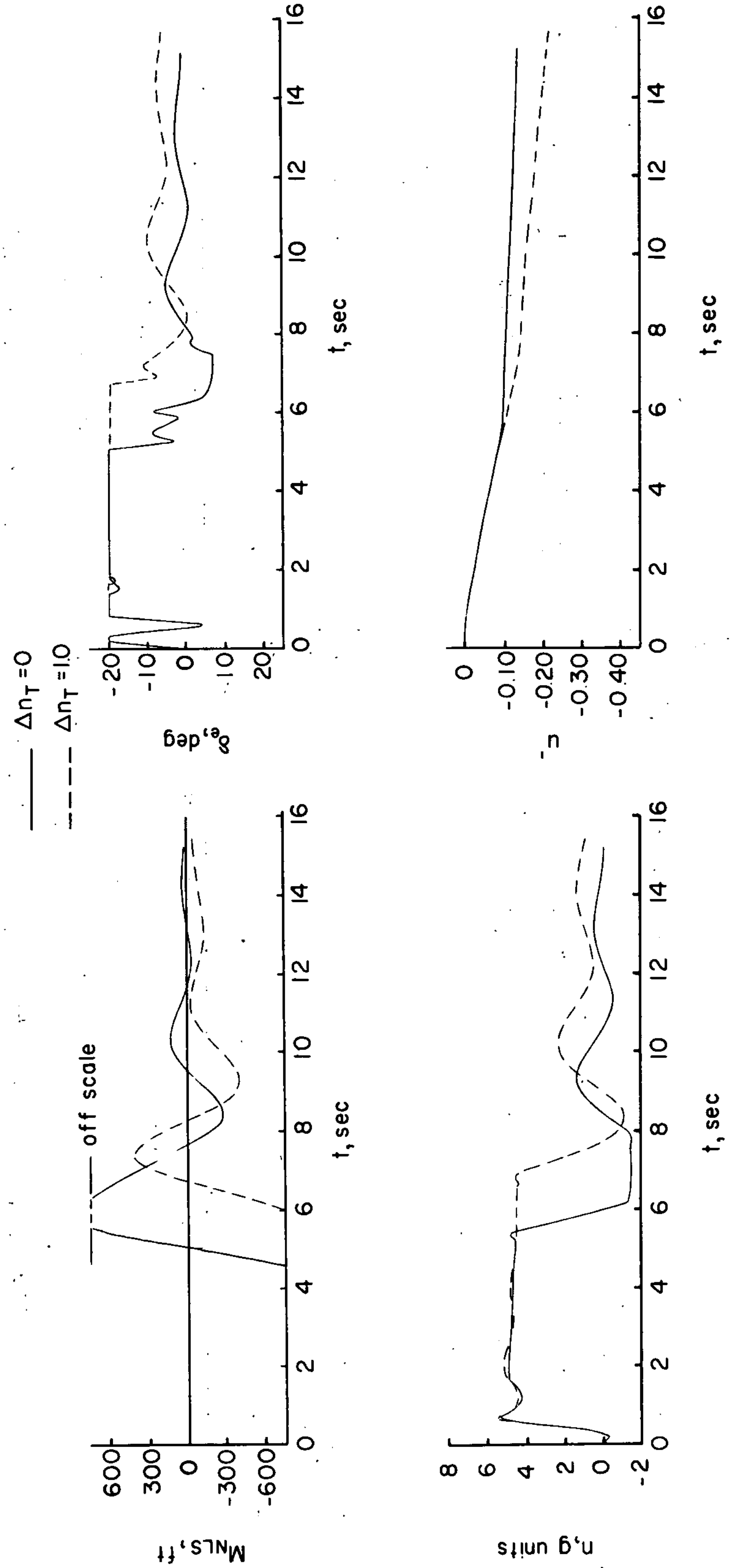

(b) $K = 200.0$; $K_1 = K_2 = 0$; $K_3 = 0.21$; $K_4 = 0$; $K_r = 2.0$.

Figure 7.- Concluded.

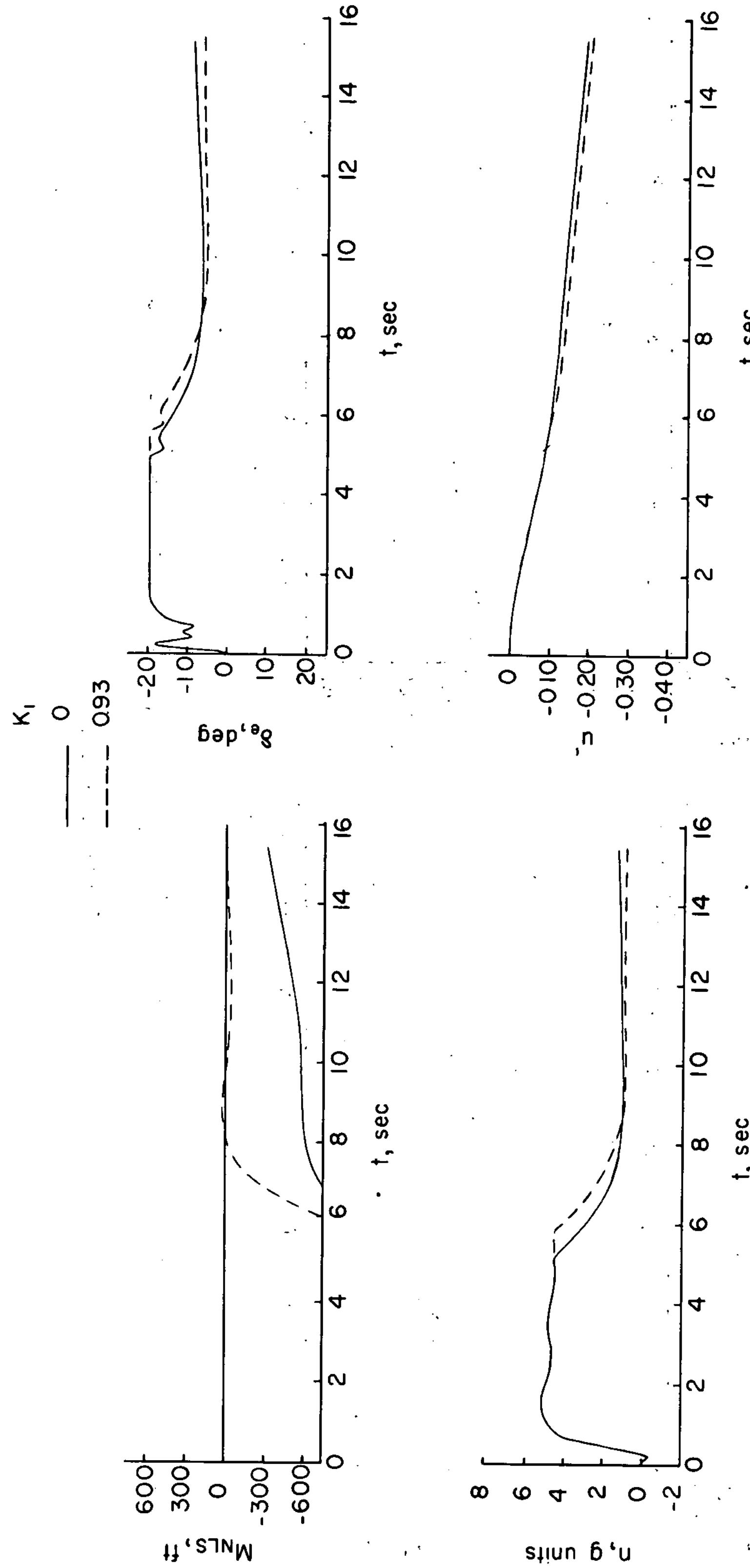

(a) $K = 33.0$; $K_2 = 0$; $K_3 = 0.21$; $K_4 = 0.30$; $K_r = 2.0$; $\Delta n_T = 1$.

Figure 8.- Effect of steering-error integration gain K_1 on interceptor attack performance. Normal-acceleration command system; $R_o = 60,000$ ft; $\sigma_o = 7.5^o$; $\gamma_{I_o} = 0$; $\gamma_{T_o} = \pi$.

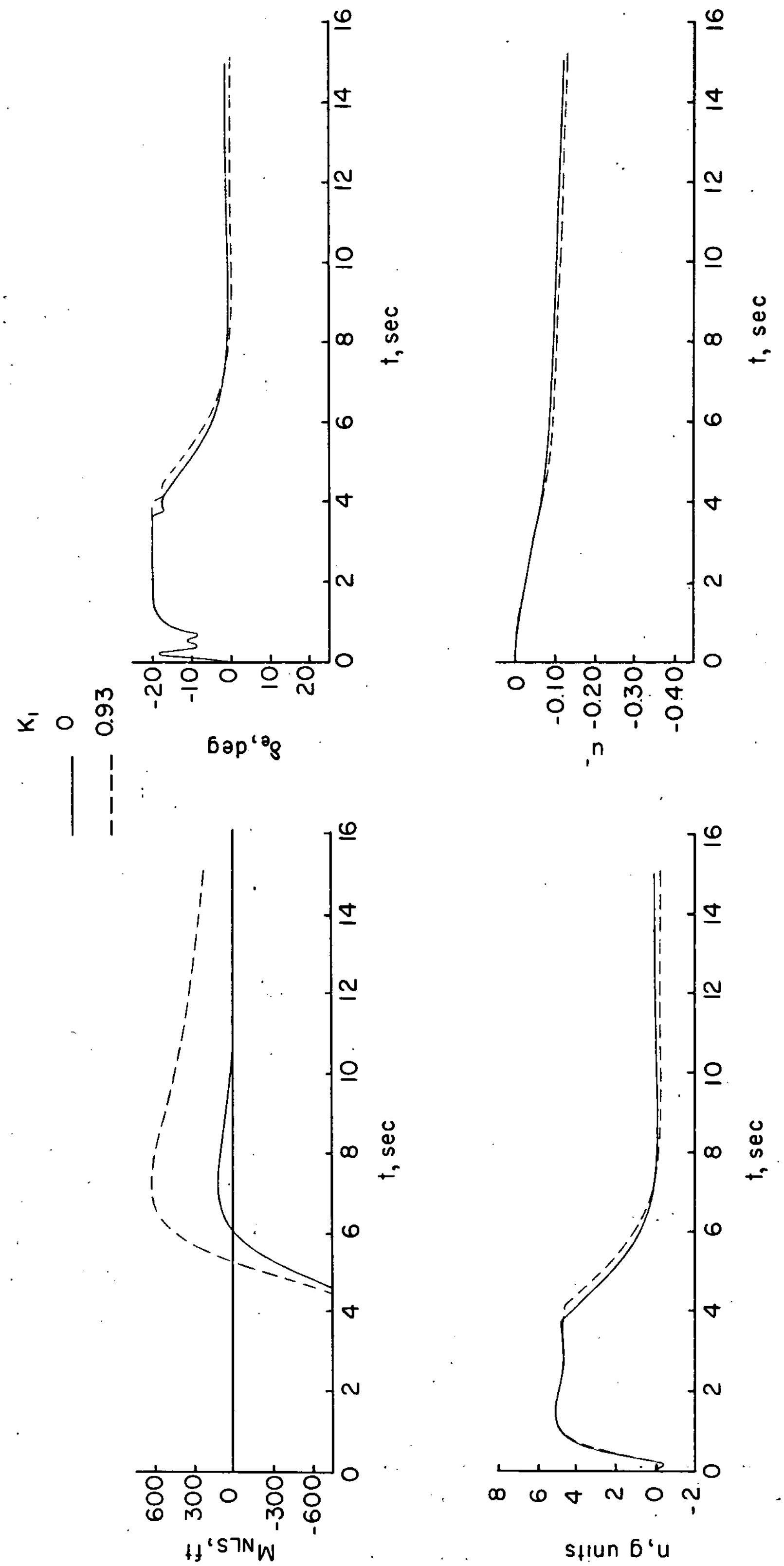

(b) $K = 33.0$; $K_2 = 0$; $K_3 = 0.21$; $K_4 = 0.30$; $K_r = 2.0$; $\Delta n_T = 0$.

Figure 8.- Concluded.

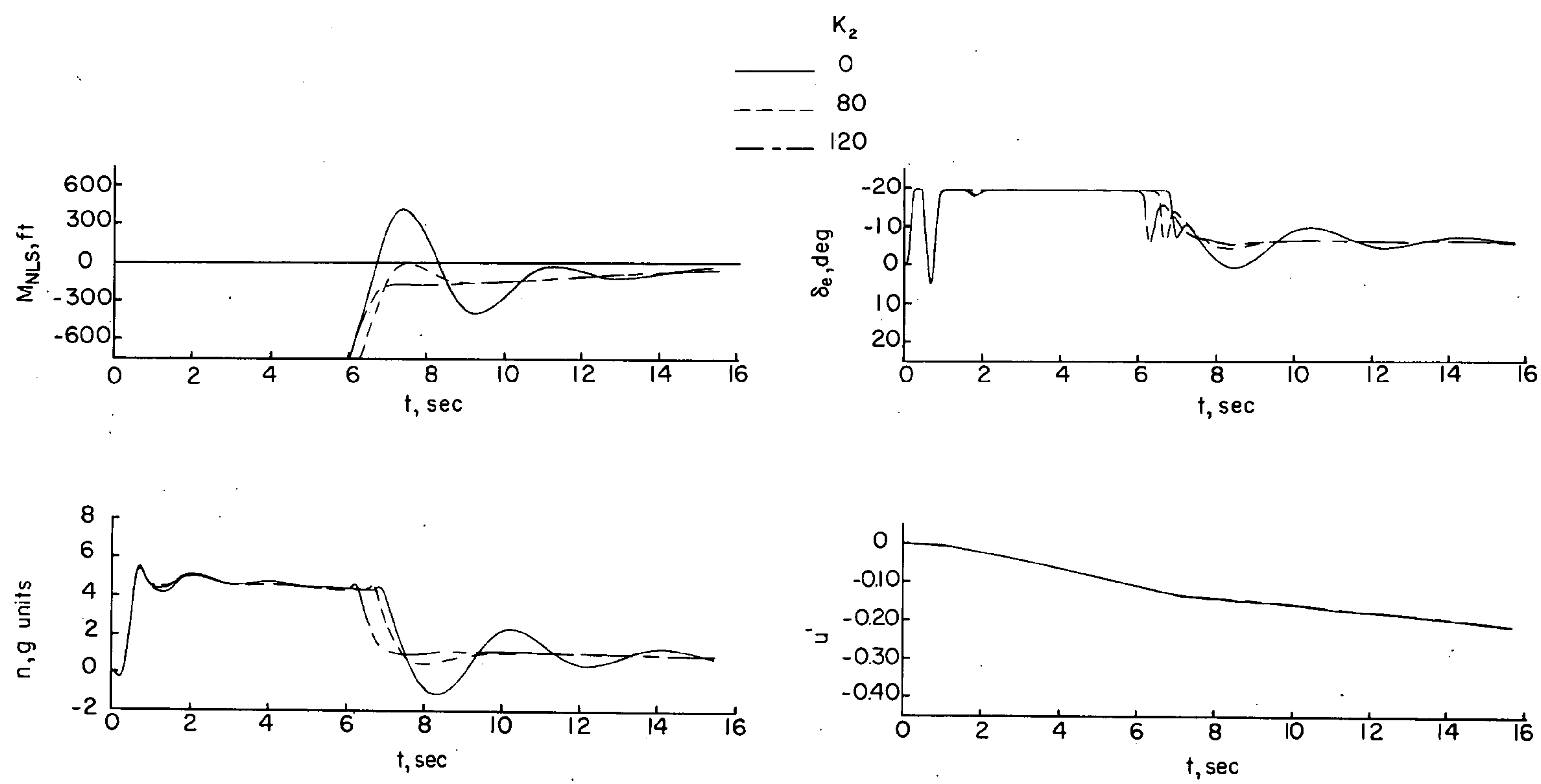

(a) $\Delta n_T = 1$.

Figure 9.- Effect of steering-error differentiation gain K_2 on interceptor attack performance. Normal-acceleration command system; $R_o = 60,000$ ft; $\sigma_o = 7.5^o$; $K = 200.0$; $K_1 = K_4 = 0$; $K_3 = 0.21$; $K_r = 2.0$; $\gamma_{I_o} = 0$; $\gamma_{T_o} = \pi$.

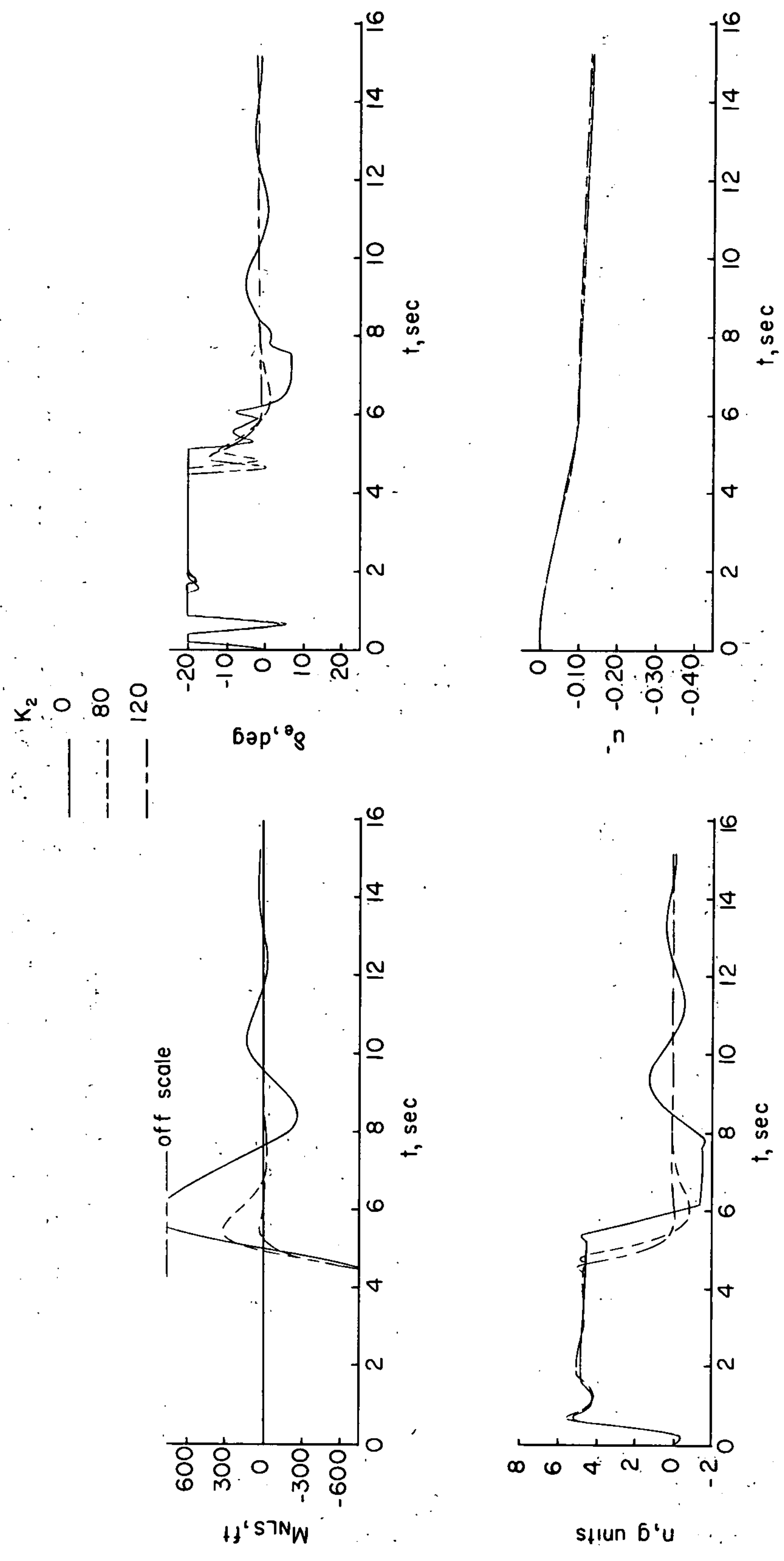

(b) $\Delta n_T = 0$.

Figure 9.- Concluded.

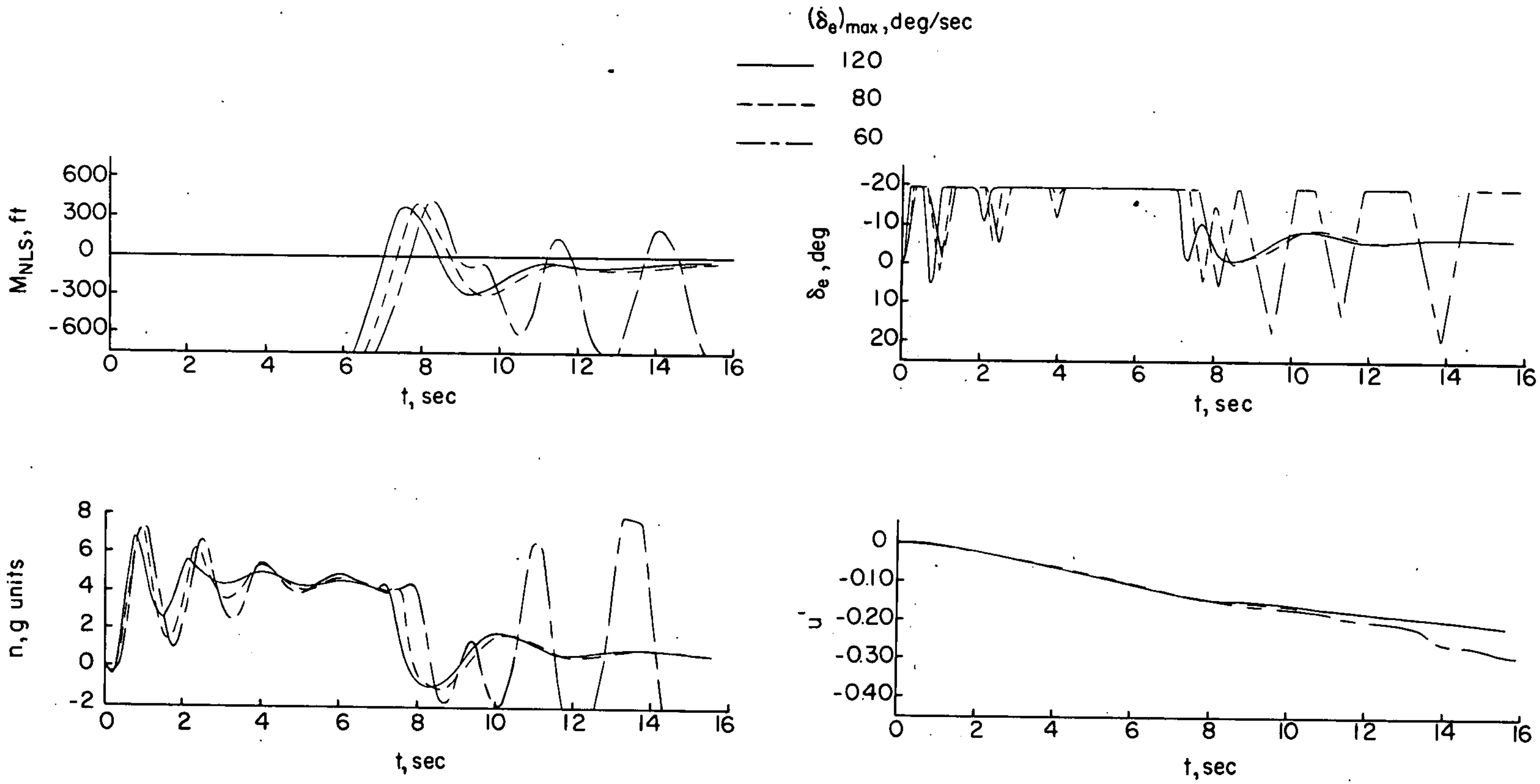

(a) $K_r = 1.0$; $K_2 = 0$.

Figure 10.- Effect of limiting rate of elevator deflection $\dot{\delta}_e$ on interceptor attack performance. Normal-acceleration command system; $R_o = 60,000$ ft; $\sigma_o = 7.5^o$; $K = 200.0$; $K_1 = K_4 = 0$; $K_3 = 0.21$; $\Delta n_T = 1$; $\gamma_{I_o} = 0$; $\gamma_{T_o} = \pi$.

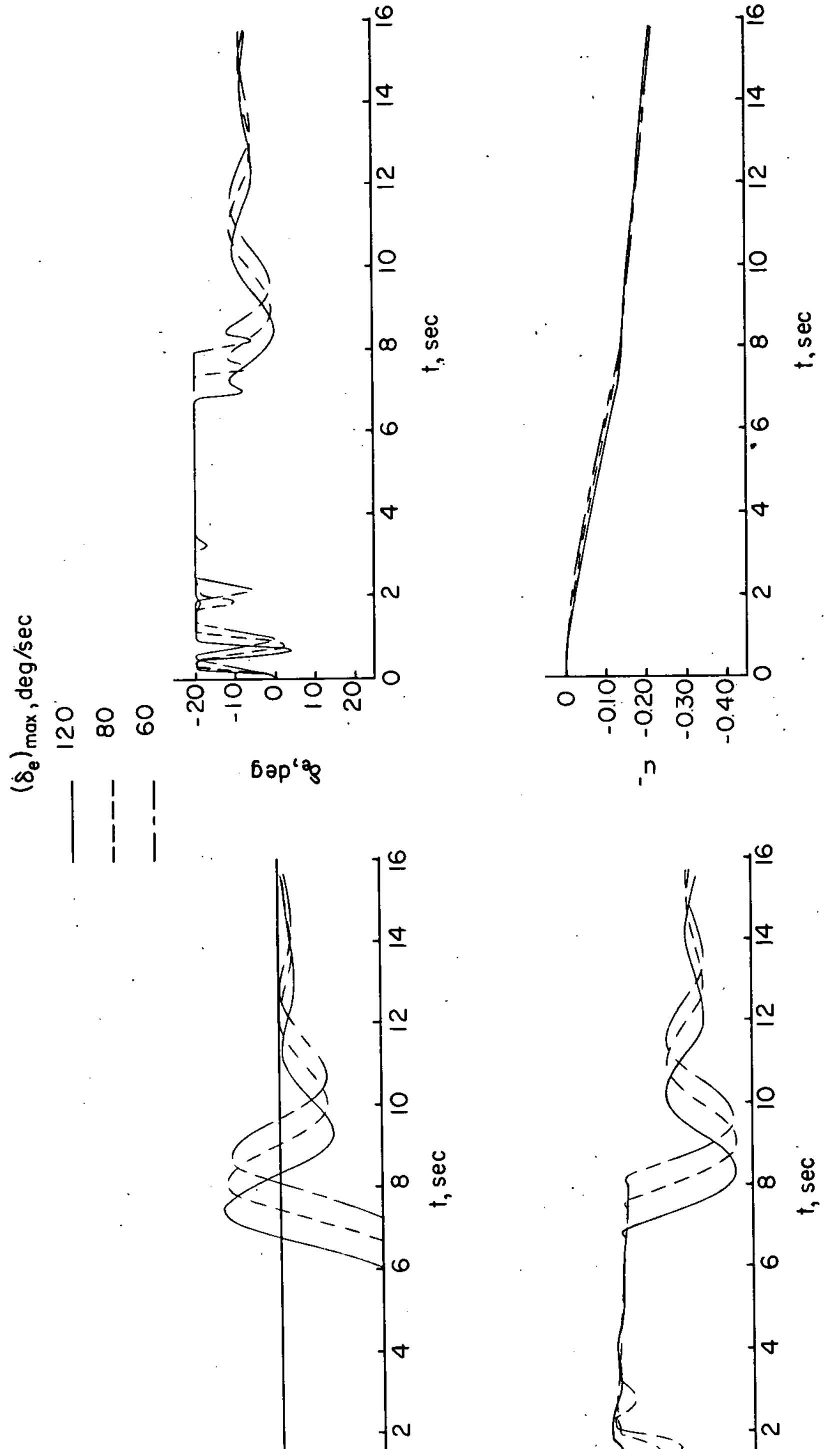

(b) $K_r = 2.0$; $K_2 = 0$.

Figure 10.- Continued.

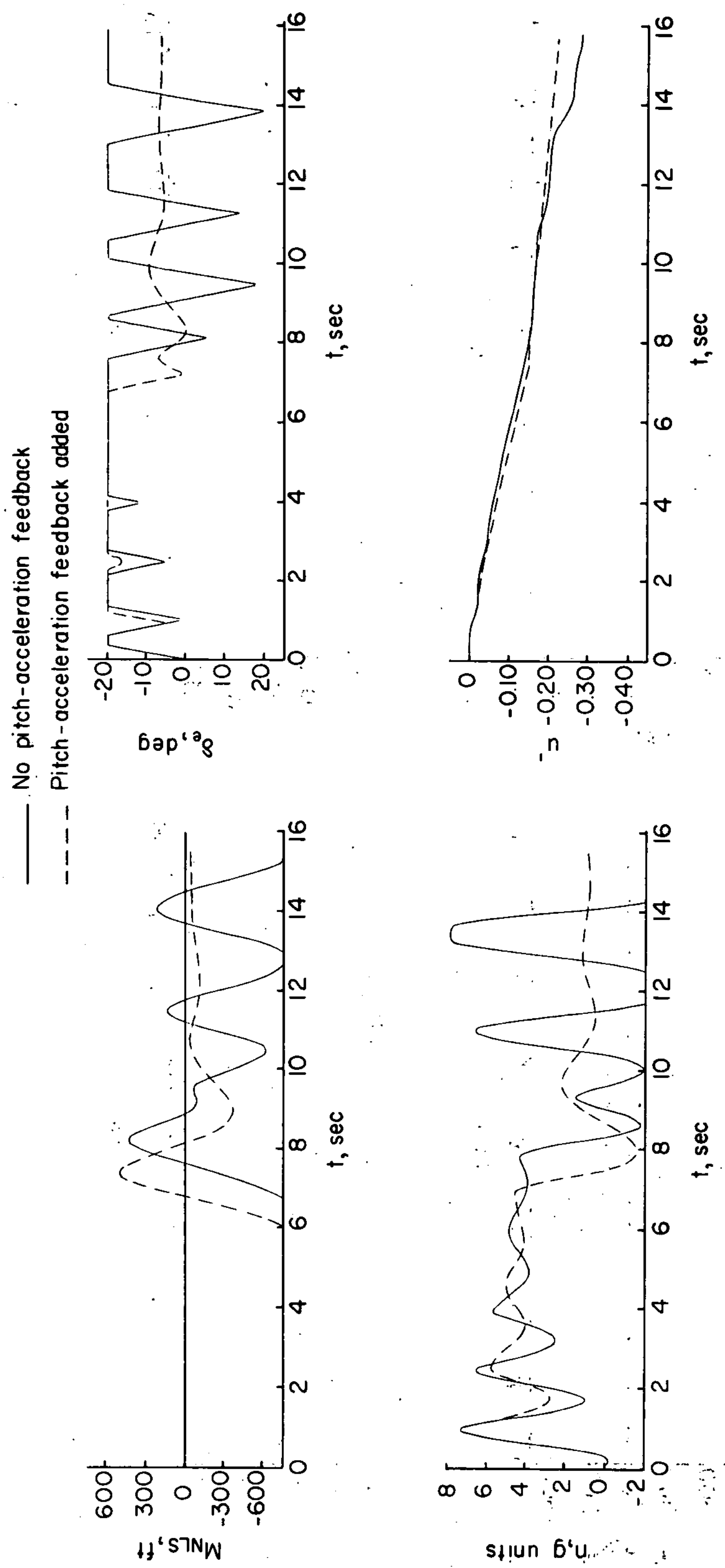

(c) $K_r = 1.0$; $K_2 = 0$; $(\dot{\delta}_e)_{max} = 60^{\circ}/sec.$

Figure 10.- Continued.

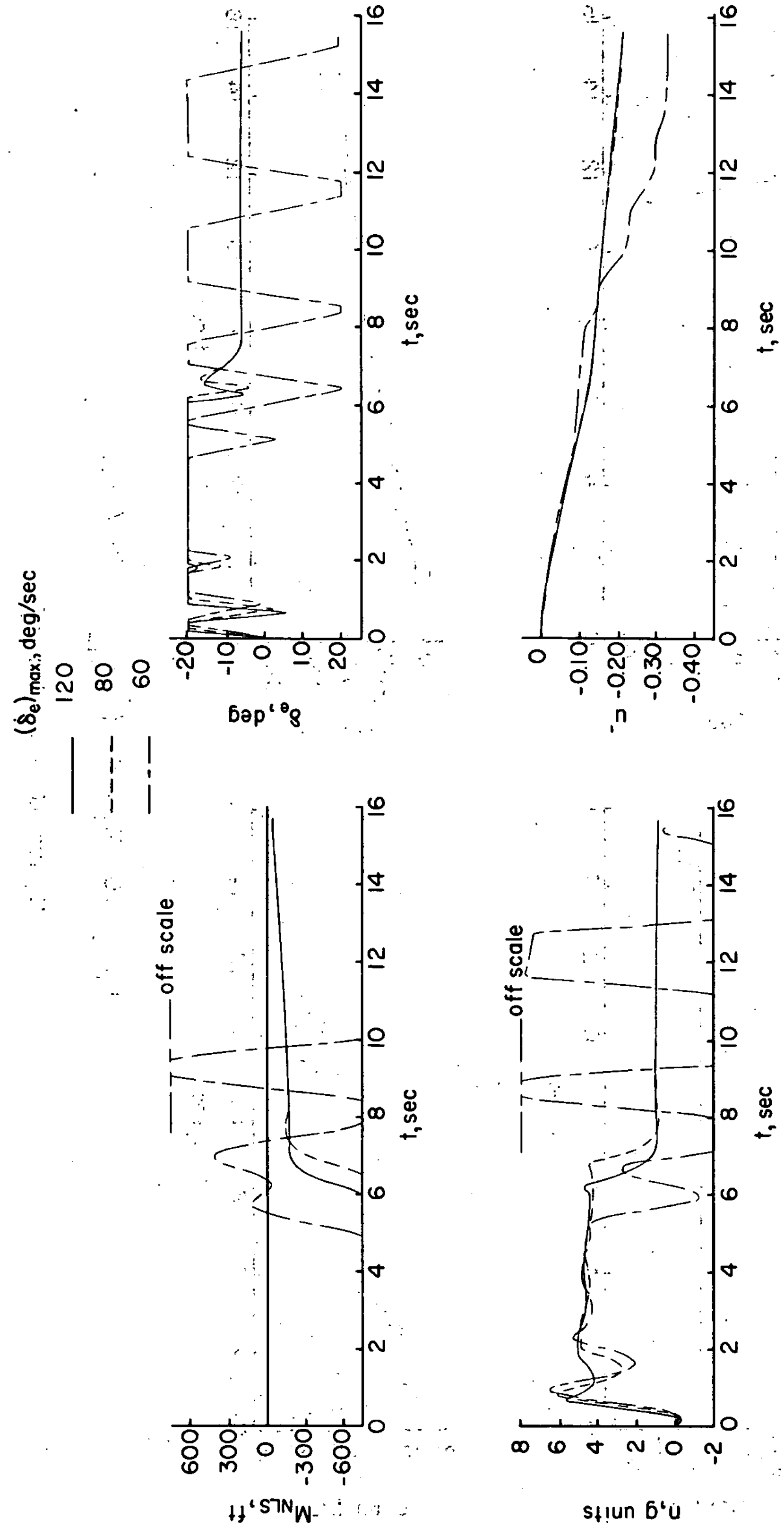

(d) $K_r = 2.0$; $K_2 = 120$.

Figure 10.- Continued.

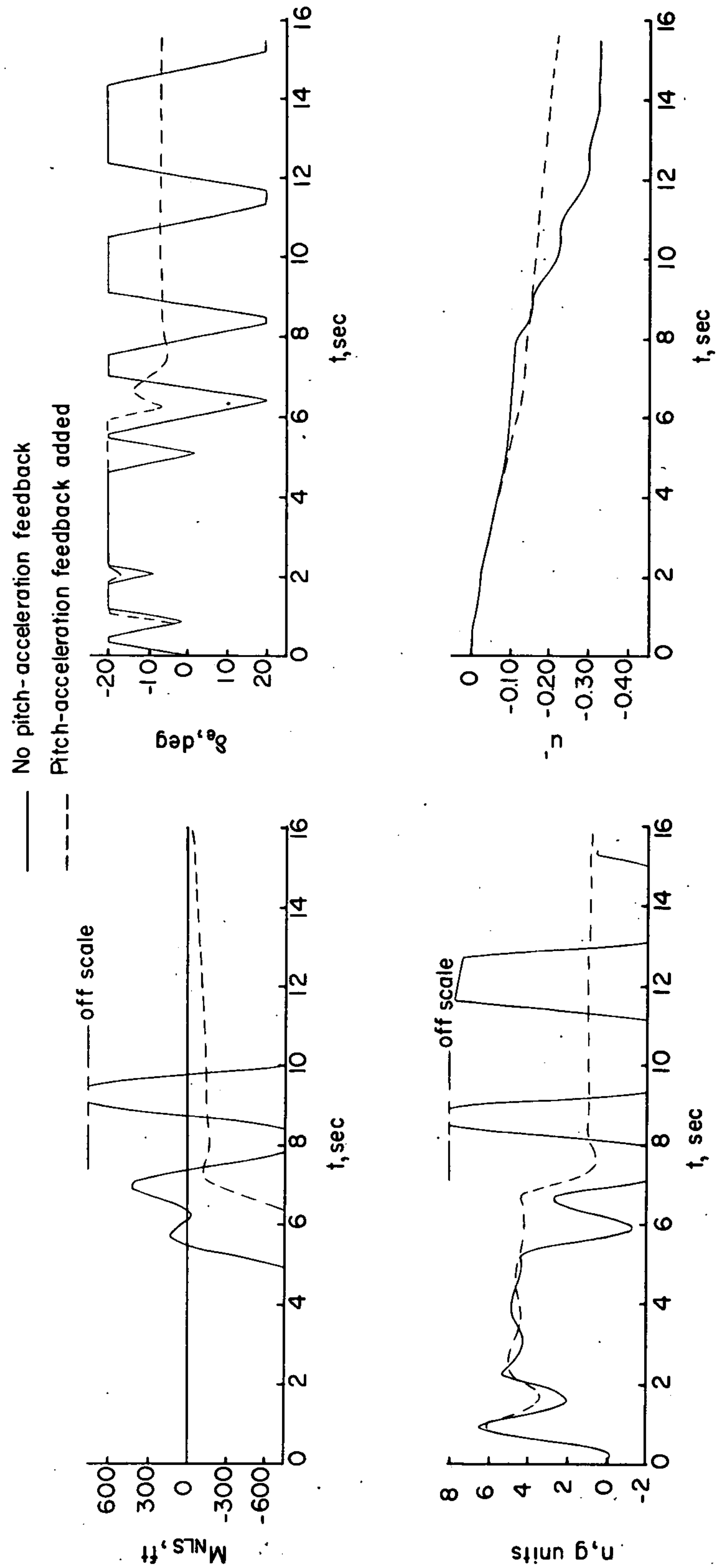

(e) $K_r = 2.0$; $K_2 = 120$; $(\dot{\delta}_e)_{max} = 60^\circ/\text{sec}$.

Figure 10.- Concluded.